NUREG/CR-0530
PNL-2870
RE
/-

Solubility Classification of Airborne Products from Uranium Ores and Tailings Piles

D. R. Kalkwarf

January 1979

Prepared for
the U.S. Nuclear Regulatory Commission
under a Related Services Agreement with
the U.S. Department of Energy
under Contract EY-76-C-06-1830

Pacific Northwest Laboratory
Operated for the U.S. Department of Energy
by Battelle Memorial Institute

Battelle

PNL-2870

NOTICE

PACIFIC NORTHWEST LABORATORY
operated by
BATTELLE
for the
UNITED STATES DEPARTMENT OF ENERGY
Under Contract EY-76-C-06-1830

Printed in the United States of America
Available from
National Technical Information Service
United States Department of Commerce
5285 Port Royal Road
Springfield, Virginia 22151

Price: Printed Copy $____*; Microfiche $3.00

*Pages	NTIS Selling Price
001-025	$4.00
026-050	$4.50
051-075	$5.25
076-100	$6.00
101-125	$6.50
126-150	$7.25
151-175	$8.00
176-200	$9.00
201-225	$9.25
226-250	$9.50
251-275	$10.75
276-300	$11.00

NUREG/CR-0530
PNL-2870
RE

SOLUBILITY CLASSIFICATION OF AIRBORNE PRODUCTS FROM URANIUM ORES AND TAILINGS PILES

D. R. Kalkwarf

January 1979

Prepared for
the U.S. Nuclear Regulatory Commission
under a Related Services Agreement
with the U.S. Department of Energy
under Contract EY-76-C-06-1830
Fin No. B21237

Pacific Northwest Laboratory
Richland, Washington 99352

SUMMARY

Airborne products generated at uranium mills were assigned solubility classifications for use in the ICRP Task Group Lung Model. Assignments were based on measurements of the dissolution half-times exhibited by their component radionuclides in simulated lung fluid at 37°C. No significant difference was seen between the dissolution behavior of airborne samples and sieved ground samples of the same product, and both types were utilized in making the assignments. If the product contained radionuclides that dissolved at different rates, composite classifications were assigned to show the solubility class of each component. If the dissolution data indicated that a radionuclide was present in two chemical forms that dissolved at different rates, a mixed classification was assigned to show the percentage of radionuclide in each solubility class. Both composite and mixed classifications were shown to be compatible with the ICRP Lung Model. Based on results from seven samples, uranium-ore dust was assigned the composite classification: (^{235}U,^{238}U) W; (^{226}Ra) 10% D, 90% Y; (^{230}Th,^{210}Pb,^{210}Po) Y. Based on the results from nine samples, tailings-pile dust was classified: (^{226}Ra) 10% D, 90% Y; (^{230}Th,^{210}Pb,^{210}Po) Y. No significant difference was seen between the dissolution behavior of tailings-pile dust from either the alkaline-leach or acid-leach process for uranium recovery. Based on the results from five samples, uranium octoxide was classified Y. Based on the results from two samples, uranium tetrafluoride was also classified Y. Based on the results from one sample, ammonium diuranate was classified D. Based on the results from five

samples, yellow-cake dust was classified (^{235}U,^{238}U) 60% D, 40% W. The term "yellow cake," however, covers a variety of materials which differ significantly in color, chemical composition, and dissolution rate; and this classification represents the average behavior of samples whose individual classifications ranged from 100% D to 36% D, 64% Y. Solubility classifications based on the dissolution half-times of particular yellow-cake products should, thus, be used when available.

CONTENTS

FIGURES

TABLES

INTRODUCTION

This study was conducted to classify the solubilities of airborne products from uranium mills in terms of the ICRP Task Group Lung Model.[1] The International Committee on Radiation Protection has recommended this model for computing the clearance rate of dust from the human respiratory tract. Thus, it provides a basis both for lung dosimetry and for setting exposure limits to airborne radioactive dusts. A key factor in this model is the clearance classification of the inhaled material. Three clearance classes were established: D, W and Y, corresponding to biological half-times of 0 to 10 days, 11 to 100 days, and >100 days, respectively. In the absence of biological data, clearance classifications for materials have been approximated by their dissolution half-times in simulated lung fluids.[1-3] Although endocytosis and ciliary-mucus transport are known to contribute to lung clearance, experiments have indicated that a few days after dust deposition, dissolution determines the clearance rate for the lower respiratory tract.[4-5]. Given material of a particular clearance or solubility class, the model assigns transport rates for this material from various anatomical compartments. From these parameters, one can compute the residence times of the material and the associated radiation dose in each compartment.

In the present study, dissolution-rate measurements were made *in vitro* but under conditions simulating those in the lung. Dissolutions were carried out at 37°C in an aqueous solution whose composition closely matched that for interstitial lung

fluid. The small amounts of protein and lipid normally present in lung fluid were omitted since their identities are not well established, and the inclusion of substitutes in the lung-fluid simulant would have created conditions for rapid bacterial growth. Maximum dissolution rates were sought because the lung was expected to be a site for efficient dissolution and because the values were to approximate clearance rates that included contributions from endocytosis and ciliary-mucus transport.

Four types of mill products were investigated: uranium-ore dust, tailings-pile dust, yellow-cake dust, and uranium tetrafluoride. The first two products are well known to be heterogeneous materials containing a variety of radionuclides that may dissolve at different rates. For such samples, dissolution rates were evaluated for five long-lived members of the ^{238}U-decay chain: ^{238}U (as traced by ^{235}U), ^{230}Th, ^{226}Ra, ^{210}Pb, and ^{210}Po. For samples of yellow cake and uranium tetrafluoride, only dissolution rates of uranium were evaluated since its isotopes were the only radionuclides present at significant concentrations. Dissolution rates of pure uranium octoxide and ammonium diuranate were also evaluated in order to check on previous classifications for these substances and to interpret the dissolution behavior of the mill products.

CONCLUSIONS AND RECOMMENDATIONS

Measurement of the half-times for dissolution of uranium-mill products into simulated lung fluid at 37°C provided a practical basis for classifying their solubilities in terms of the ICRP Task Group Lung Model. If the products contained

several radionuclides that dissolved at different rates, this behavior was summarized by composite classifications showing the solubility class of each component. When the decrease in amount of undissolved radionuclide could not be described by a single exponential function in time, the sum of two exponential terms was found adequate. The latter situation indicated that the radionuclide was present in two chemical forms with significantly different dissolution rates, and the product was assigned a mixed classification showing the percentage of radionuclide in each solubility class. No significant difference was seen between the dissolution behavior of airborne samples and sieved ground samples of the same product, and no significant difference was seen between the dissolution behavior of tailings dust from mills using either the alkaline-leach or acid-leach process for uranium recovery. No significant change was seen in the dissolution properties of tailings dust with distance from the piles, up to 500 meters.

Recommended solubility classifications for the products examined in this study are:

uranium-ore dust:	(^{235}U,^{238}U) W; (^{226}Ra) 10% D, 90% Y; (^{230}Th,^{210}Pb,^{210}Po) Y
tailings-pile dust:	(^{226}Ra) 10% D, 90% Y; (^{230}Th,^{210}Pb, ^{210}Po) Y
uranium octoxide:	Y
uranium tetrafluoride.	Y
ammonium diuranate:	D
yellow-cake dust:	(^{235}U,^{238}U) 60% D, 40% W

The term "yellow cake," however, was found to apply to materials

with significantly different chemical structure, and the solubility classification recommended above is a generalization of the behavior of the samples examined. When available, solubility classifications based on the dissolution half-times of particular products should be used.

EXPERIMENTAL

COLLECTION OF SAMPLES

Samples of uranium ore dust were collected from the air around ore-crushing operations and from deposits of dust on horizontal structural elements at these sites. Airborne samples were collected on glass fiber filters mounted in high-volume air samplers. The filters were rated by the manufacturer as 99.9% efficient in removing 0.3 μm aerosols of dioctyl phthalate in the DOP-retention test. They were changed daily, and the dust collected on successive days was composited until at least 4 grams were obtained. Samples of deposited dust were obtained simply by sweeping portions into a container.

Samples of yellow-cake dust were collected both from the air near drying operations and from production lots submitted for analysis. The latter were furnished by the Sequoyah Laboratory, Kerr-McGee Nuclear Corporation, Gore, Oklahoma, and included samples from the Anaconda Corporation mill at Blue Water, New Mexico, the Exxon Minerals Company mill at Casper, Wyoming, the United Nuclear-Homestake Partners mill at Milan, New Mexico, and the Kerr-McGee Nuclear Corporation mill at Ambrosia Lake, New Mexico. A sample of airborne yellow cake was also obtained at the latter mill. This was collected with a high-volume air

sampler near a vent of exhaust air from the yellow-cake drying operation.

Tailings-pile dust was collected at the three mills in New Mexico listed above. Samples were collected both directly on the tailings piles and at sites considered to be at the perimeters of the tailings-pile areas. On the piles themselves, samples were collected from both ground-surface deposits and from air impact flow particle collectors[6] left at the sites for the months of April and May. A diagram of this type of collector is shown in Figure 1. Particles enter through a 7.6-cm diameter inlet and collect at the bottom of a 25-cm diameter nylon screen. Sample collection at these sites was attempted with high-volume air samplers, but due to calm air, insufficient sample was obtained in even a 5-day sampling period. Only the air impact flow particle collectors were used at the perimeter sites. At Mill 1, the sampling site was on a perimeter road approximately 500 meters from the edge of the tailings pile but still 1000 meters within mill property. At Mill 3, this site was on the actual mill boundary, approximately 100 meters from the edge of the tailings pile. At Mill 4, the sampling site was also approximately 100 meters from the edge of the tailings pile on a road defining the pile boundaries but still 500 meters within mill property. In each case, the particle collectors were positioned downwind from the prevailing wind across the tailings piles.

Other uranium compounds were obtained from various sources. Uranium tetrafluoride was obtained from the Sequoyah Facility, Kerr-

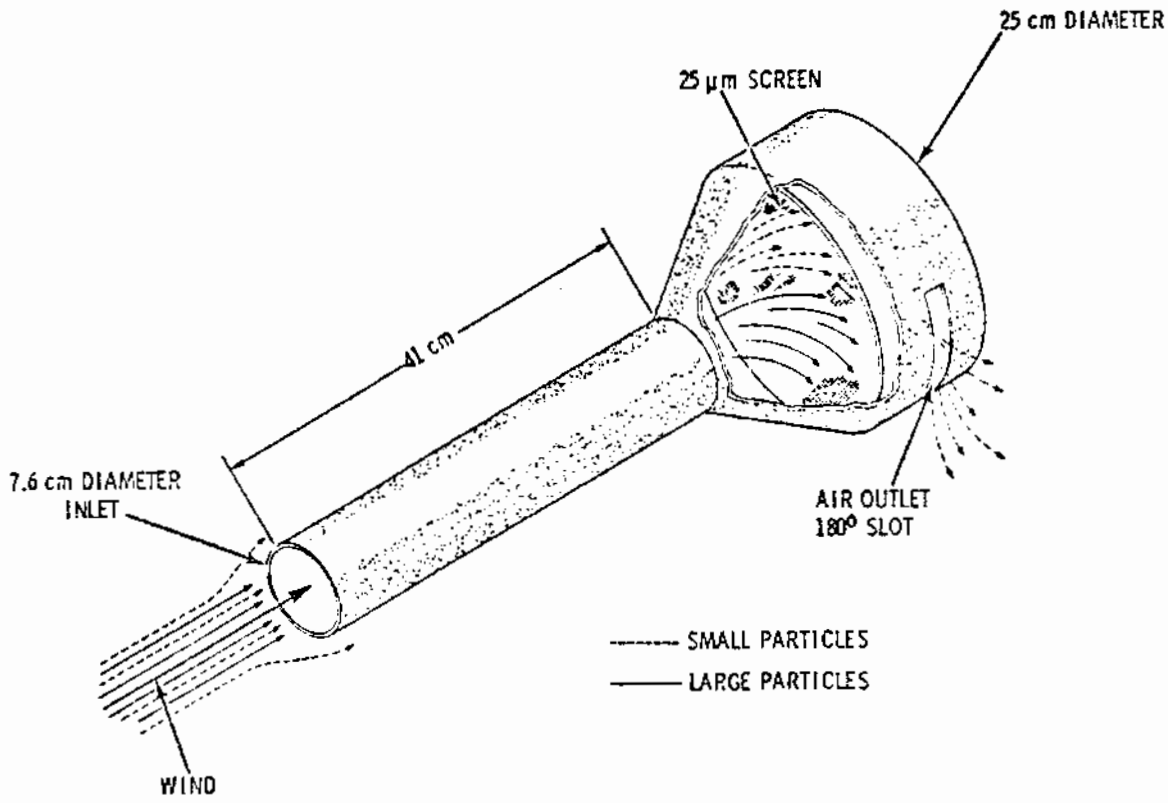

FIGURE 1. Air Impact Flow Particle Collector

McGee Nuclear Corporation, Gore, Oklahoma, and from the Metropolis Works, Allied Chemical Corporation, Metropolis, Illinois. A sample of ammonium diuranate was obtained from the Westinghouse Corporation, Nuclear Fuels Division, Columbia, South Carolina. One sample of uranium octoxide was obtained from the U. S. National Bureau of Standards as reference material SRM-950. Four others were produced by heating samples of the four commercial yellow-cake products to constant weight at 800°C.

DETERMINATION OF PARTICLE SIZE AND AREA

Samples were sieved prior to surface-area and dissolution-rate determinations, and unless otherwise specified, only particles that passed through a 325 mesh U. S. Standard Sieve with 45-μm aperatures were used. Some samples were separated with a Bahco Microparticle Classifier into fractions with narrow particle-size ranges in order to test for possible correlation between dissolution rate and particle size. Due to the irregular shapes of the particles, however, dissolution rates were expected to correlate more closely with the specific surface areas of the samples. These were measured by the B.E.T. method[7], using a Micromeritics Surface Area Analyzer. In this method, an inert gas is allowed to interact with the sample until a monomolecular layer of gas is adsorbed on its surface. The specific surface area is then calculated from the volume of gas adsorbed, its molecular diameter, and the weight of the sample. Since the gas molecules are small compared to any irregularities in the surface of the particles, this method provides a much more accurate measure of specific surface area than could be calculated from particle-size distributions.

PREPARATION OF SIMULATED LUNG FLUID

Simulated lung fluid with the composition shown in Table 1 was used in this study. This composition was recommended by Moss[8] after a comparison of various media simulating interstitial fluids. It was achieved by slowly adding the following ingredients in order to 990 ml of distilled water and adjusting the final volume to 1000 ml:

0.2033 g $MgCl_2 \cdot 6H_2O$
6.0193 g NaCl
0.2982 g KCl
0.2680 g $Na_2HPO_4 \cdot 7H_2O$
0.0710 g Na_2SO_4
0.3676 g $CaCl_2 \cdot 2H_2O$
0.9526 g $NaH_3C_2O_2 \cdot 3H_2O$
2.6043 g $NaHCO_3$
0.0970 g $Na_3H_3C_6O_7 \cdot 2H_2O$

If the pH of the resulting solution was not 7.3, it was adjusted to this value with small volumes of 1 N HCl.

TABLE 1. Compositions of Actual and Simulated Lung Fluids

Ion	Actual[9]		Simulated[8]	
Calcium, Ca^{2+}	5.0	meq/ℓ	5.0	meq/ℓ
Magnesium, Mg^{2+}	2.0	"	2.0	"
Potassium, K^{+}	4.0	"	4.0	"
Sodium, Na^{+}	145.0	"	145.0	"
Total Cations	156.0	"	156.0	"
Bicarbonate, HCO_3^{-}	31.0	"	31.0	"
Chloride, Cl^{-}	114.0	"	114.0	"
Citrate, $H_3C_6O_7^{3-}$	--		1.0	"
Acetate, $H_3C_2O_2^{-}$	7.0	"	7.0	"
Phosphate, HPO_4^{2-}	2.0	"	2.0	"
Sulfate, SO_4^{2-}	1.0	"	1.0	"
Protein	1.0*	"	---	
Total Anions	156.0	"	156.0	"
pH	7.3		7.3	

*Assuming meq protein/ℓ = 4.15 (g protein/ℓ).

MEASUREMENT OF RADIONUCLIDES

Radionuclides in dust samples were assayed both by gamma-ray spectrometry and by alpha-energy analysis following chemical separation. In the gamma-ray analyses, the counting rates for the 46.5 keV photon of ^{210}Pb, the 68.0 keV photon of ^{230}Th, the 163 keV photon of ^{235}U, and the 186 keV photon of ^{226}Ra were measured. For ore dust, ±10% precision was generally achieved by counting 4-gram samples on a 1-inch diameter intrinsic germanium diode for 4 hours. A similar precision was achieved by counting 15-gram samples of tailings dust on a 2-inch diameter intrinsic germanium diode for from 4 to 18 hours.

The chemical separation techniques were those developed in this laboratory for routine analyses of uranium ores and tailings-pile material. Briefly, a solid sample was dissolved in acid and measured amounts of ^{232}U, ^{234}Th, ^{208}Po, and ^{133}Ba were added as internal standards. In one aliquot of this solution uranium and thorium were separated from the other nuclides by coprecipitation on calcium phosphate. This precipitate was then dissolved, and the uranium and thorium were separated by selective extraction into a solution of 10% dihydroxyaluminum aminoacetate in xylene. Aqueous solutions of the separated radionuclides were prepared, each was electroplated on a separate metal disc, and the deposited radionuclides were counted on an alpha-energy analyzer.

A second aliquot of the dissolved sample was used to evaluate the ^{210}Po, ^{210}Pb, and ^{226}Ra content. A measured amount of ^{208}Po was added as an internal standard, and the aliquot was

made 0.4 N in hydrochloric acid. Ascorbic acid and ethylenediaminetetraacetic acid were added to complex interfering ions, the polonium was allowed to plate out on a silver disc, and the disc was counted on an alpha-energy analyzer. The same method was used to determine the amount of ^{210}Po dissolved in samples of simulated lung fluid.

A measured amount of ^{212}Pb was added to the solution remaining from the ^{210}Po-deposition, and lead was selectively extracted with a solution of 1% diethylammonium diethyldithiocarbamate in chloroform. It was then back-extracted into aqueous media, and the 0.239 keV photon of ^{212}Pb was counted in order to compute the chemical yield. A measured amount of ^{208}Po was then added, and the sample was set aside for about 100 days in order to let ^{210}Po build in. At the end of this time, the polonium nuclides were allowed to plate out on a silver disc and counted on an alpha-energy analyzer. The amount of ^{210}Pb in the sample was computed using both these measurements and the time allowed for ^{210}Po ingrowth.

Radium-226 in the aqueous layer remaining from the lead extraction was separated from uranium and thorium by converting the latter elements to their anionic chloride complexes and re-removing them on an anion-exchange resin. Cation radionuclides in the filtrate were then adsorbed on a column of cation-exchange resin, calcium was eluted with ammonium acetate, and both ^{226}Ra and ^{133}Ba were eluted with nitric acid. The samples were dried at 400°C to remove ammonium acetate and then counted on a total alpha counter for ^{226}Ra. The samples were also counted in a 7-inch sodium iodide well-crystal for ^{133}Ba in order to compute

the chemical yield. The same method was used to determine the amount of ^{226}Ra dissolved in samples of simulated lung fluid.

Rapid spectrophotometric methods were developed to assay samples of simulated lung fluid exposed to uranium compounds. Amounts of hexavalent uranium were evaluated from direct measurements on filtered lung fluid in 10-cm cells at 448 nm. The optical absorbance at this wavelength was found to increase linearly with uranium concentration, as confirmed independently by Davies-Gray redox titrations. The precision of the method was estimated to be ±5%. Mixed amounts of tetravalent and hexavalent uranium were evaluated by oxidizing all uranium in the fluid to the hexavalent state with periodic acid. Typically, 3 grams of periodic acid were dissolved in 100 ml of sample, the temperature was raised to 80°C for one minute, and the recooled solution was examined in 10-cm cells at 425 nm. Again, the optical absorbance at this wavelength was found to increase linearly with uranium concentration, and the precision of the method was estimated to be ±5%.

DISSOLUTION OF SAMPLES

Two dissolution methods were used: the batch method and the pass-by method. In the batch method, the dust particles were contacted with simulated lung fluid at 37°C for a selected period of time, the two phases were separated rapidly by filtration, and either the solid residue or the filtrate was assayed for radionuclide content. The solid residue was then recontacted with fresh fluid, and the procedure was repeated. Millipore HA filters with 0.45 μm size pores were generally used to separate the

phases, but Millipore VF filters with 0.01 μm size pores were also used to test for incomplete phase separation. Four-gram samples of ore dust were suspended in 200 ml of simulated lung fluid contained within a closed Pyrex flask and the contents were agitated with a motor-driven Teflon paddle. The same system was utilized for dissolution of tailings dust except that 15-gram samples of dust were used. For dissolution of yellow cake and other uranium compounds, 0.6-gram samples were added to 100-ml aliquots of simulated lung fluid in closed Pyrex flasks, and the contents were agitated on a motor-driven shaker-bath. In all cases, the pH of the solution was monitored at least weekly and adjusted to 7.3 with dilute hydrochloric acid, if necessary.

In the pass-by method, simulated lung fluid at 37°C was continuously passed by a bed of dust particles enclosed between Millipore VF filters. This sample packet is shown in Figure 2 and consisted of a weighed amount of sample enclosed by filters that were sealed to a Teflon-ring spacer with rubber cement. It was placed in the bottom section of a polypropylene dissolution chamber shown in Figure 3 and compressed with the polyethylene-screen end of the middle core. The upper section of the chamber was then added, and all external seams were sealed with ethylene dichloride which acted as a solvent for the plastic. The leak-tight chamber, fitted with silicone rubber tubing at the inlet and outlet was immersed in a water bath at 37°C, and simulated lung fluid was pumped through the chamber with a peristaltic pump. The incoming fluid passed down the center of the

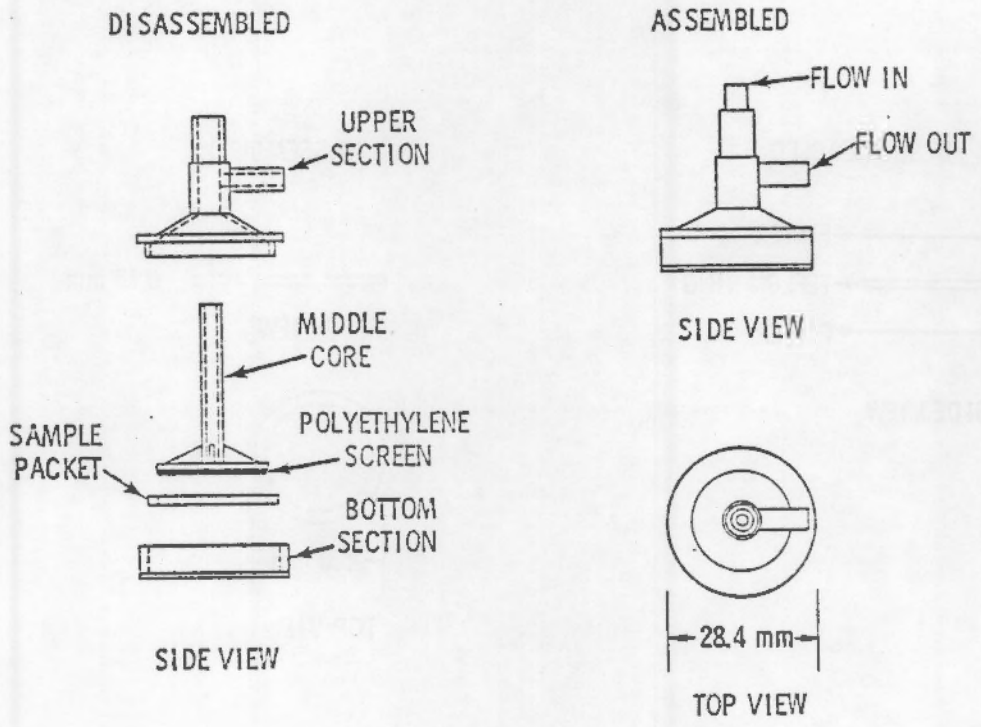

FIGURE 2. Sample Packet for the Pass-by Dissolution Chamber

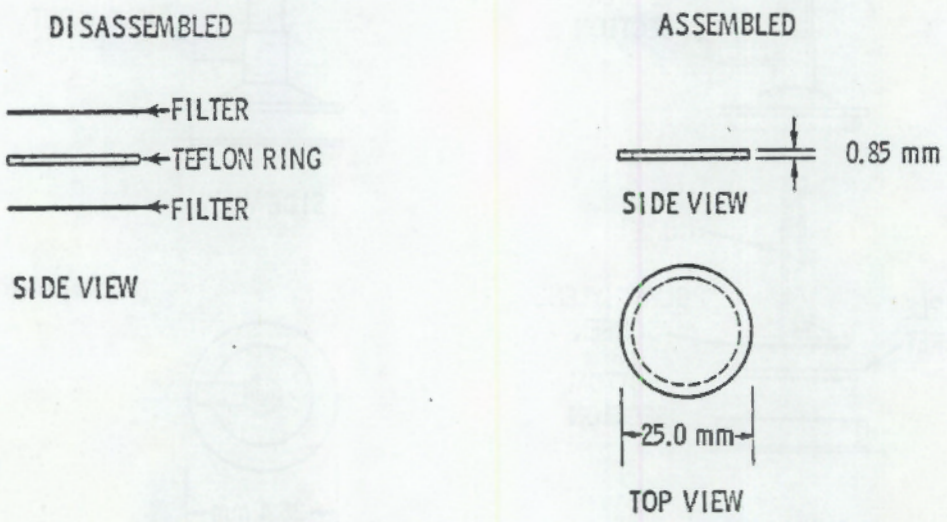

FIGURE 3. Pass-by Dissolution Chamber

middle core, radially across the upper surface of the packet to the periphery, and then around the outside of the middle core to the outlet. By increasing the flow rate, the dissolution process could also be increased by enhancing the diffusion rate of dissolved material from the interior of the sample bed to the filter at the surface. The contents of the dissolution chamber could be assayed rapidly for residual gamma-emitting radionuclides by removing it from the bath and placing it on a 1-inch diameter intrinsic germanium diode.

RESULTS

COMPARISON OF DISSOLUTION METHODS

The batch and pass-by methods of dissolution were compared in order to decide which could be used most easily to obtain data for the evaluation of maximum dissolution rates. The dissolution rate of a pure substance has been shown to be proportional to the surface area of the solid phase in contact with the solvent and to the difference between the concentration of dissolved substance at equilibrium (the solubility) and the concentration near the solid surface at any earlier time.[10] To attain maximum dissolution rates in the present study, the latter concentration was kept as small as possible. In the batch method, this was done by continuously shaking or stirring the dust particles and periodically replacing the liquid phase with fresh solvent. In the pass-by method, it was done by increasing the flow rate of solvent past the particles. Results from four dissolution trials on the same yellow-cake material are compared in Figure 4. It was apparent that impractically

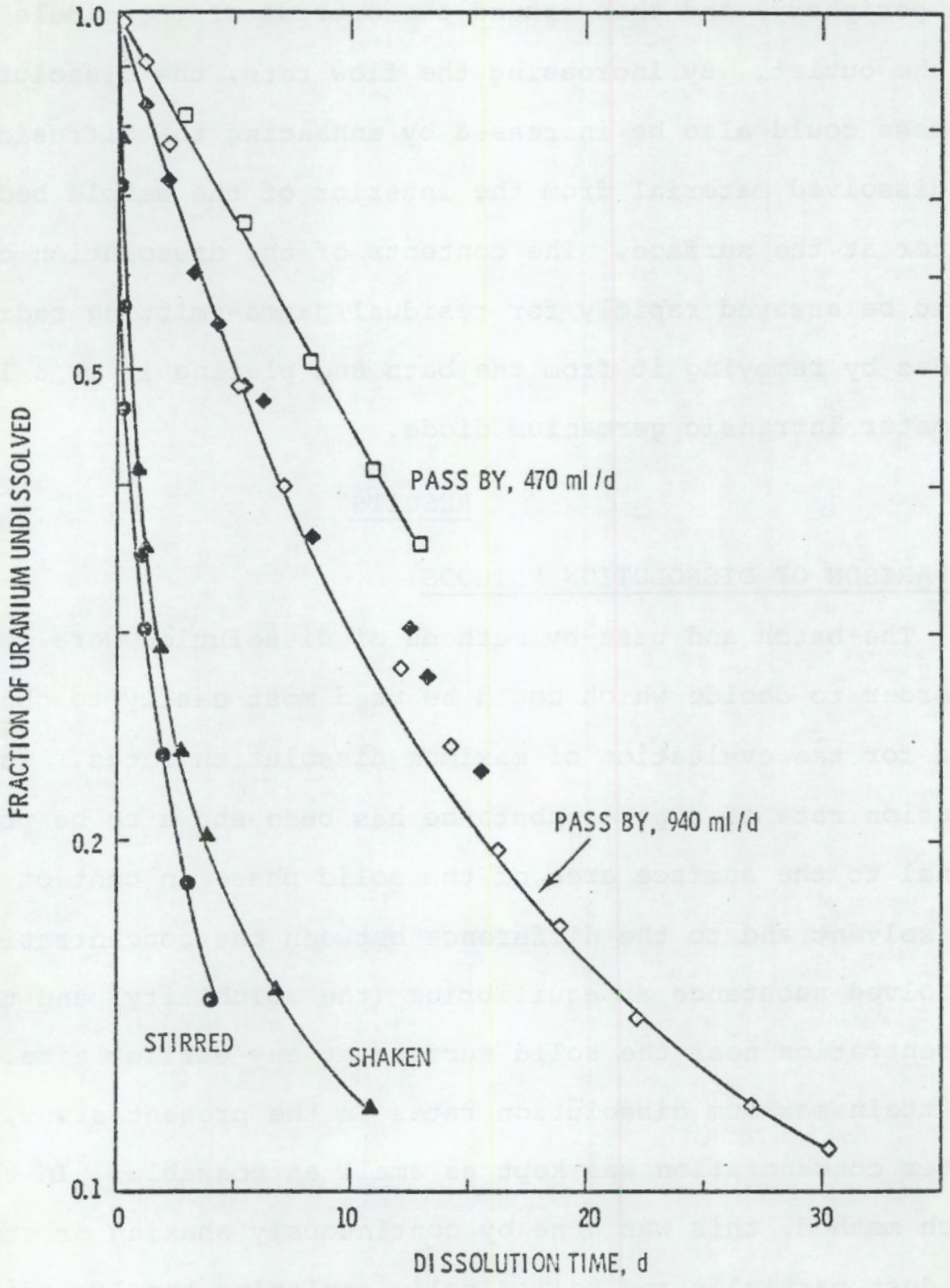

Figure 4. Dissolution of Yellow Cake as a Function of Agitation. Open symbols indicate values obtained by gamma counting whereas filled symbols indicate values obtained from spectrophotometric data.

high flow rates of solvent would have to be sent through the pass-by dissolution chamber in order to evaluate maximum dissolution rates of a material that dissolved this rapidly. As a result, the batch method was used for all other dissolution-rate evaluations. The test also showed that measurements of the amount of uranium remaining undissolved by both direct counting and by spectrophotometric analysis of the aqueous phase were in good agreement.

DISSOLUTION OF YELLOW-CAKE DUST

Dissolution half-times for production samples of yellow cake from each of four mills were evaluated. The fractions of uranium remaining undissolved after various time periods are shown in Figure 5. In each case, these fractions were found to be expressed by the sum of two exponential terms,

$$F = F_1 \exp\left[-0.693t/(t_{0.5})_1\right] + F_2 \exp\left[-0.693t/(t_{0.5})_2\right].$$

The two exponential terms were resolved by graphical analysis, and the dissolution half-times, together with their 90% confidence intervals, were computed by linear regression analysis. The results are tabulated in Table 2, along with other properties of the samples.

Uranium analyses were provided with the production samples, but supplementary assays for NH_4^+, SO_4^{-2}, ^{230}Th, and ^{226}Ra were also of interest in order to assess the composition of the yellow-cake samples and the radiological hazard from their uranium daughters. NH_4^+ was evaluated by the Nessler procedure, SO_4^{-2} was evaluated gravimetrically as $BaSO_4$ and ^{230}Th and

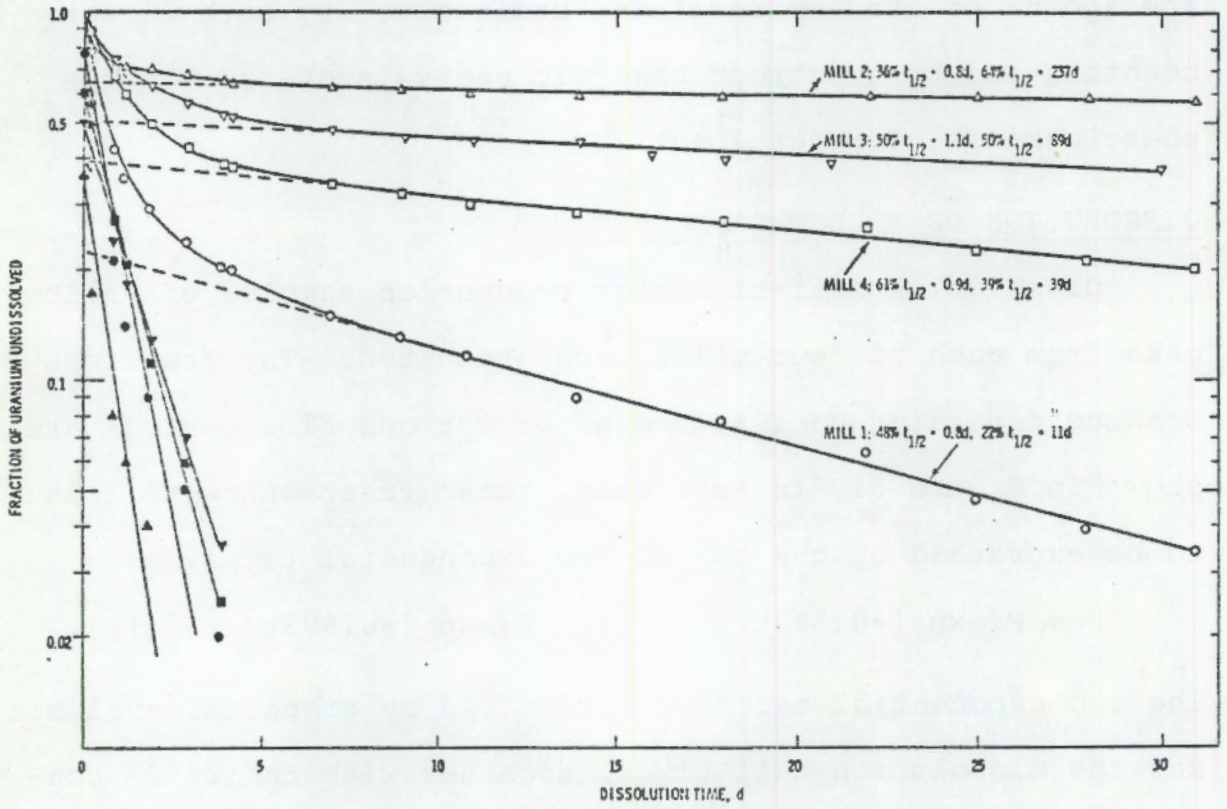

FIGURE 5. Dissolution of Yellow-cake Production Samples. Open symbols indicate experimental data whereas filled symbols indicate contributions of short-lived components.

^{226}Ra were measured by alpha counting following radiochemical separation. The results are shown in Table 3.

TABLE 2. Physical Properties and Dissolution Parameters[a] of Yellow-Cake Dust From Product Samples

Source	Area	Color	F_1	$(t_{0.5})_1$	F_2	$(t_{0.5})_2$
Mill 1	$9.4 m^2 g^{-1}$	Yellow	0.78	0.8 d (0.5-1.5)[b]	0.22	11 d (11-12)
Mill 2	15.4	Black	0.36	0.8 d (0.4-0.9)	0.64	237 d (213-267)
Mill 3	7.8	Brown	0.50	1.1 d (0.7-2.2)	0.50	89 d (79-100)
Mill 4	5.7	Orange	0.61	0.8 d (0.8-0.9)	0.39	39 d (27-69)

[a] Values are given to express the fraction of undissolved uranium as $F = F_1 \exp [-0.693t/(t_{0.5})_1] + F_2 \exp [-0.693t/(t_{0.5})_2]$.

[b] Parentheses enclose the 90% confidence limits for the dissolution half-times, $(t_{0.5})_i$.

TABLE 3. Chemical Analyses of Yellow-Cake Product Samples

Source	% U	% NH_4	% SO_4	$^{230}Th/^{238}U$[a]	$^{226}Ra/^{238}U$[b]
Mill 1	71.67	2.02	1.07	0.0088	0.00048
Mill 2	78.60	0.32	6.57	0.0015	0.00009
Mill 3	76.29	1.74	2.74	0.033	0.0095
Mill 4	77.28	2.60	3.13	0.00086	0.00011

[a] These values are for the ratio, d/m ^{230}Th:d/m ^{238}U.

[b] These values are for the ratio, d/m ^{226}Ra:d/m ^{238}U.

The variation of dissolution rate with particle size was determined on yellow-cake dust from Mill 4. Three fractions with particle size ranges 1 to 3 μm, 7 to 13 μm, and 18 to 44 μm were allowed to dissolve in separate containers of simulated

lung fluid, and the results are shown in Figure 6. Again, the data were found to be expressed by the sum of two exponential functions, and values for the relevant parameters are listed in Table 4.

TABLE 4. Surface Area and Dissolution Parameters[a] of Sized Yellow-Cake Dust

Diameter	Area	F_1	$(t_{0.5})_1$	F_2	$(t_{0.5})_2$
1-3 μm	4.7 m^2g^{-1}	0.65	1.3 d (1.3-1.4)[b]	0.35	51 d (49-53)
7-13 μm	4.3	0.60	1.3 d (1.3-1.4)	0.40	62 d (56-67)
18-44 μm	3.4	0.40	0.9 d (0.8-0.9)	0.60	89 d (84-95)

[a] Values are given to express the fraction of undissolved uranium as $F = F_1 \exp [0.693t/(t_{0.5})_1] + F_2 \exp [-0.693t/(t_{0.5})_2]$.

[b] Parentheses enclose the 90% confidence limits for the dissolution half-times, $(t_{0.5})_i$.

One sample of airborne yellow-cake dust was collected at Mill 4. In contrast to the production sample from the mill, it was yellow rather than orange and had a specific surface area of 11.4 m^2g^{-1} rather than 5.7. It was also allowed to dissolve in simulated lung fluid, and the results are shown in Figure 7. F, the fraction of uranium remaining undissolved after t days, could be expressed by the function, $F = 0.82 \exp [-0.693t/0.2] + 0.18 \exp [-0.693t/3.0]$. The 90% confidence intervals for the dissolution half-times of the two components were 0.22 to 0.24 d and 2.98 to 3.03 d, respectively.

None of the yellow-cake samples changed color during the dissolution process.

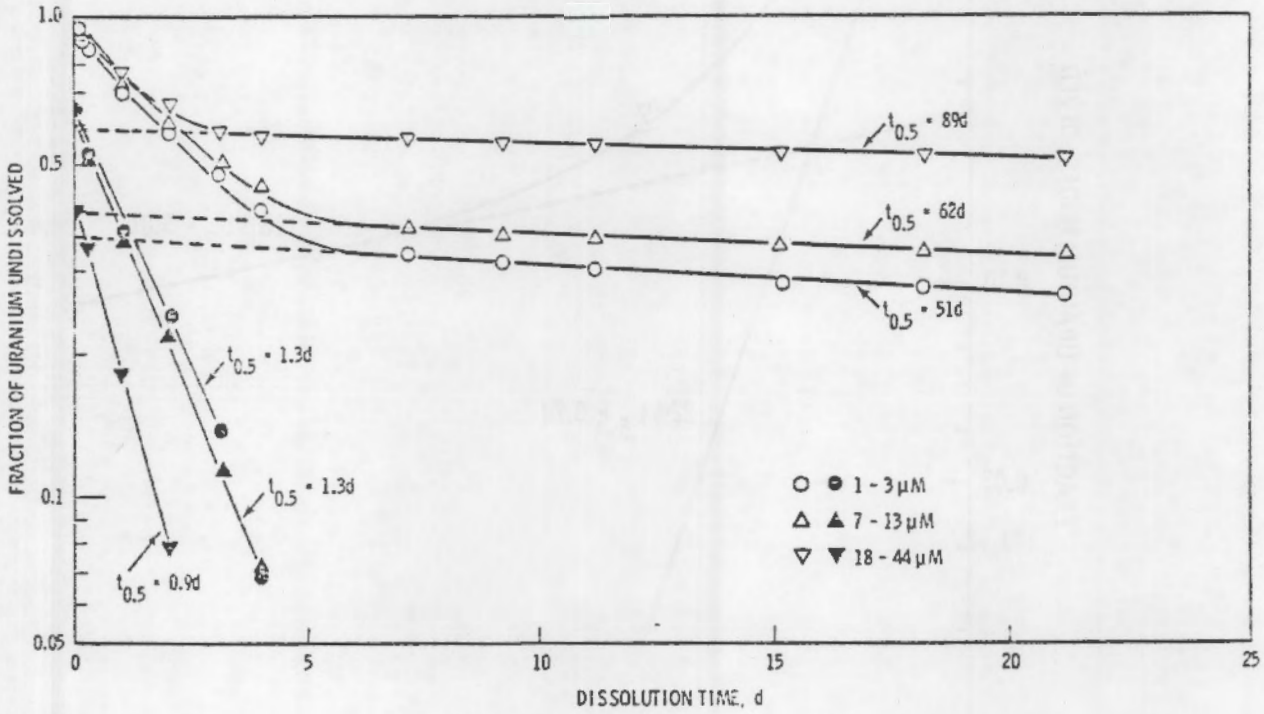

FIGURE 6. Dissolution of Yellow Cake as a Function of Particle Size. Open symbols indicate experimental data whereas filled symbols indicate contributions of short-lived components.

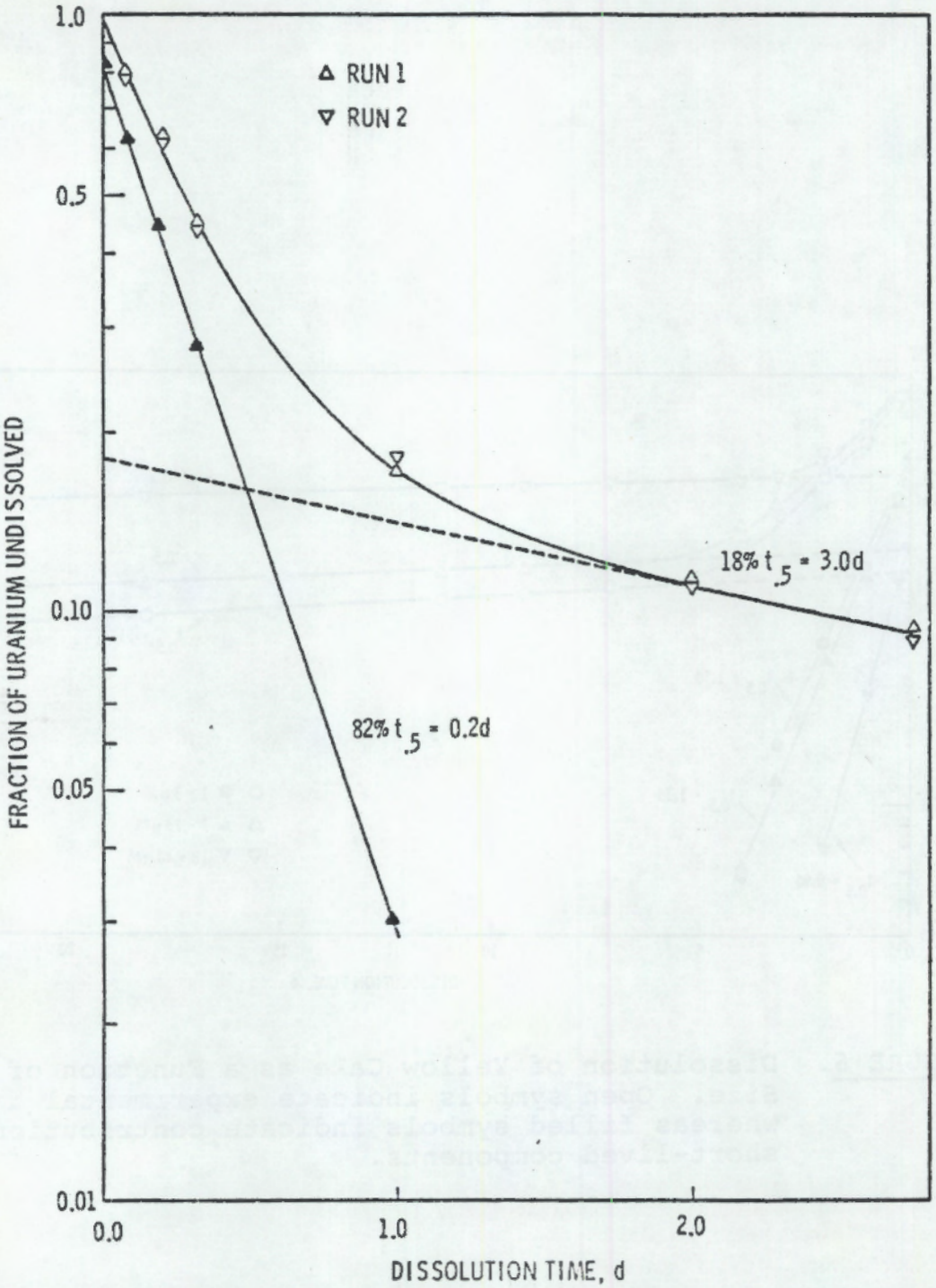

FIGURE 7. Dissolution of Airborne Yellow Cake. Open symbols indicate experimental data whereas filled symbols indicate contributions of short-lived component.

DISSOLUTION OF URANIUM OCTOXIDE AND AMMONIUM DIURANATE

Dissolution rates for five samples of uranium octoxide were evaluated. Four of these were obtained by heating yellowcake product dust, and the fifth was U. S. National Bureau of Standards SRM-950. The results are shown in Figure 8. Again, the fraction of uranium remaining undissolved was found to be represented by the sum of two exponential terms; but in each case, the short-lived component amounted to less than 10% of the total sample. Values for the relevant parameters are shown in Table 5.

TABLE 5. Dissolution Parameters[(a)] of Uranium Octoxide Dust

Source	F_1	$(t_{0.5})_1$	F_2	$(t_{0.5})_2$
Mill 1	0.08	2.0 d (1.8-2.1)	0.92	577 d (533-630)
Mill 2	0.04	2.6 d (1.6-6.6)	0.96	866 d (770-990)
Mill 3	0.08	2.7 d (1.9-4.4)	0.92	433 d (408-462)
Mill 4	0.09	3.6 d (3.3-3.9)	0.91	165 d (161-169)
NBS	0.03	4.3 d (3.6-5.5)	0.97	630 d (578-693)

(a) Values are given to express the fraction of undissolved uranium as $F = F_1 \exp [-0.693t/(t_{0.5})_1] + F_2 \exp [-0.693t/(t_{0.5})_2]$.

(b) Parentheses enclose the 90% confidence intervals for the dissolution half-times $(t_{0.5})_i$.

A sample of pure ammonium diuranate was divided into two fractions with different particle-size ranges, 125 to 250 μm and <125 μm; and each was dissolved in simulated lung fluid. The samples were found to contain 74.59% uranium compared with

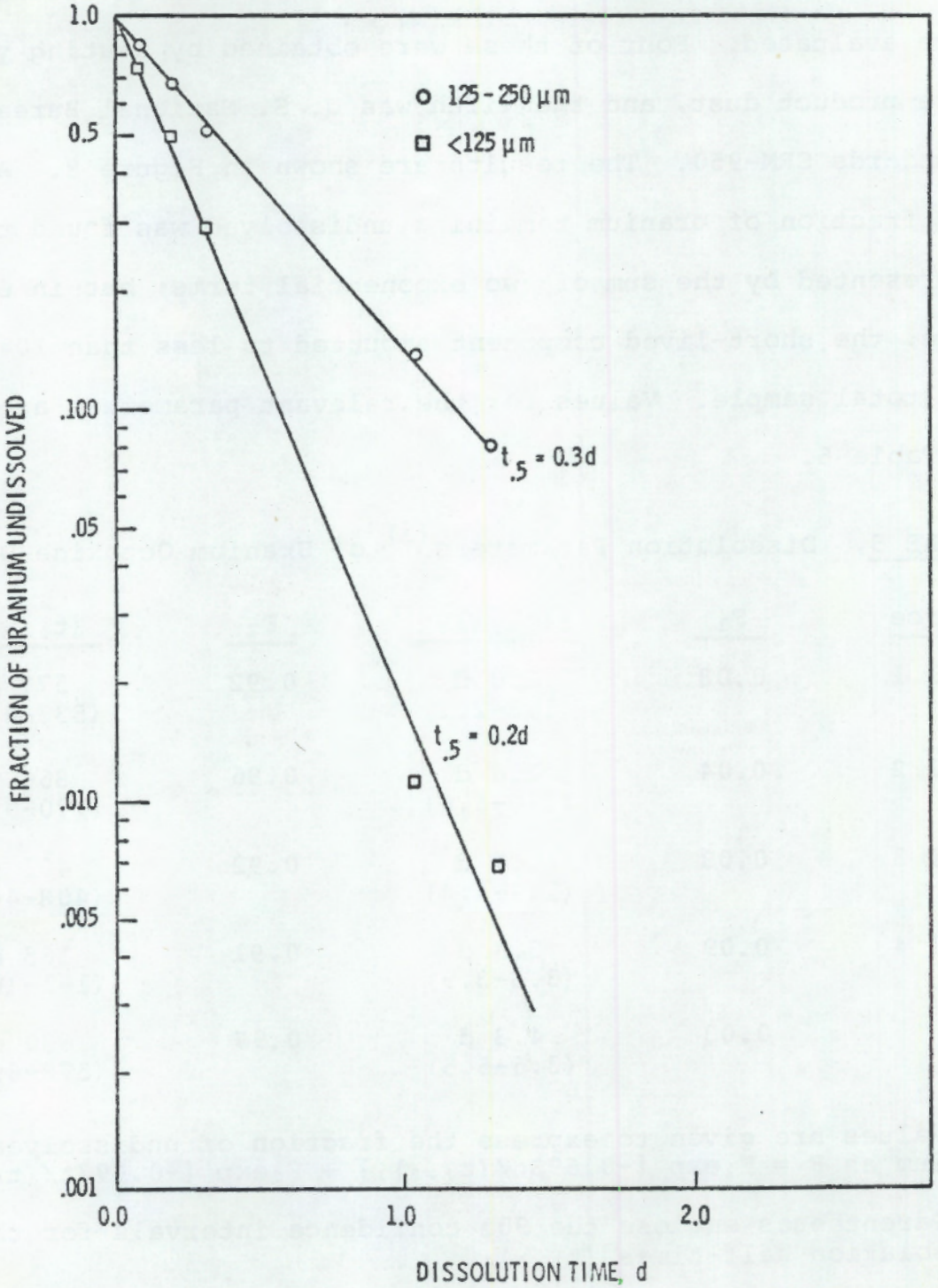

FIGURE 8. Dissolution of Ammonium Diuranate

a value of 76.28% uranium for the theoretical structure, $(NH)_4U_2O_7$. The data are shown in Figure 9; and in both cases, the fraction of uranium remaining undissolved was found to be represented by a single exponential term. Values for the relevant parameters are shown in Table 6.

TABLE 6. Physical Properties and Dissolution Parameters[a] of Ammonium Diuranate Samples

Size	Area	Color	$t_{.5}$
<125 μm	16.4 m^2g^{-1}	Yellow	0.2 d (0.16-0.19)[b]
125-150 μm	15.1	Yellow	0.3 d (0.30-0.36)

[a] Values are given to express the fraction of undissolved uranium as $F = F_1 \exp [-0.693t/(t_{0.5})_1] + F_2 \exp [-0.693t/(t_{0.5})_2]$.

[b] Parentheses enclose the 90% confidence intervals for the dissolution half-time.

DISSOLUTION OF RADIONUCLIDES FROM URANIUM-ORE DUST

The dissolution rates of ^{235}U, ^{230}Th, ^{226}Ra, ^{210}Pb, and ^{210}Po from seven samples of uranium-ore dust were evaluated. Of these, three were airborne samples collected with high-volume air samplers, and the other four were samples of dust deposited on the ground. The specific activities of the radionuclides remaining undissolved after successive periods of time are shown in Figures 10 through 16. Generally, these activities decreased exponentially with time; but for four of the samples, the data for ^{226}Ra were better expressed by the sum of two exponential terms. Values for these parameters and the specific surface areas of the samples are listed in Table 7. It was noted that

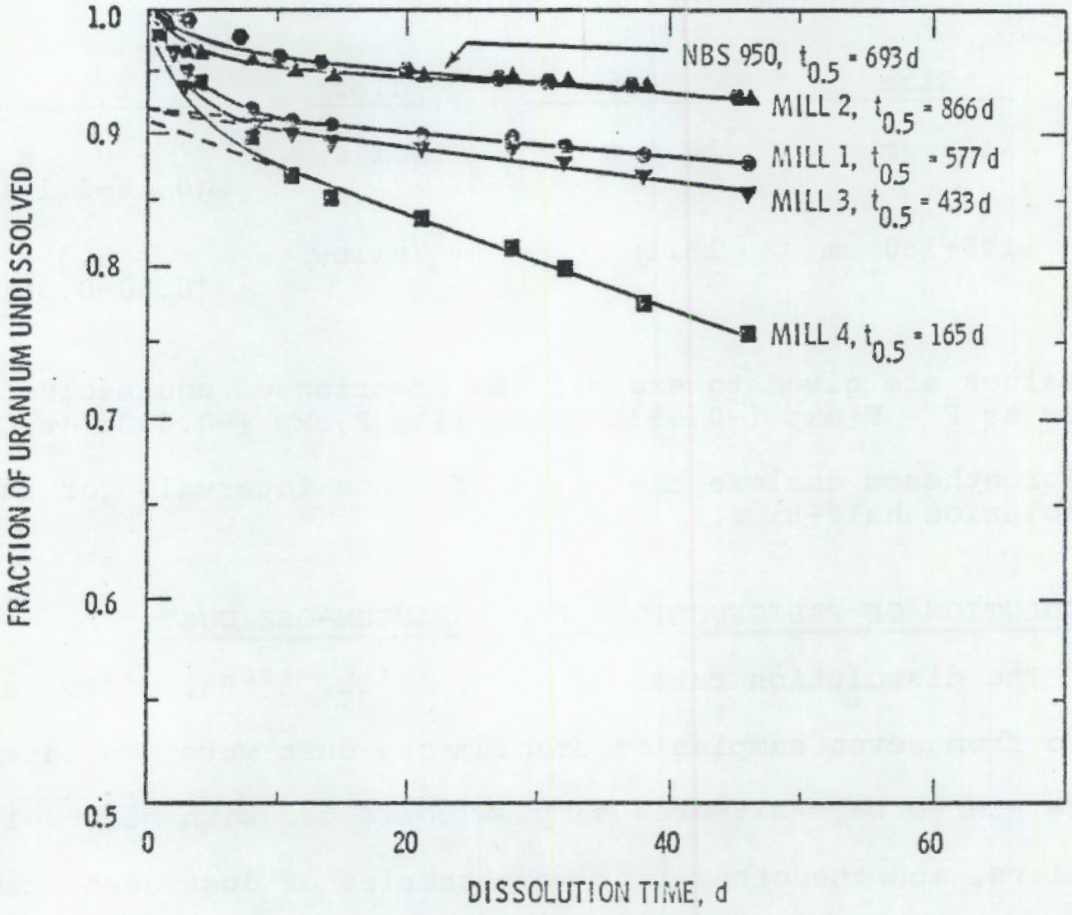

FIGURE 9. Dissolution of Uranium Octoxide

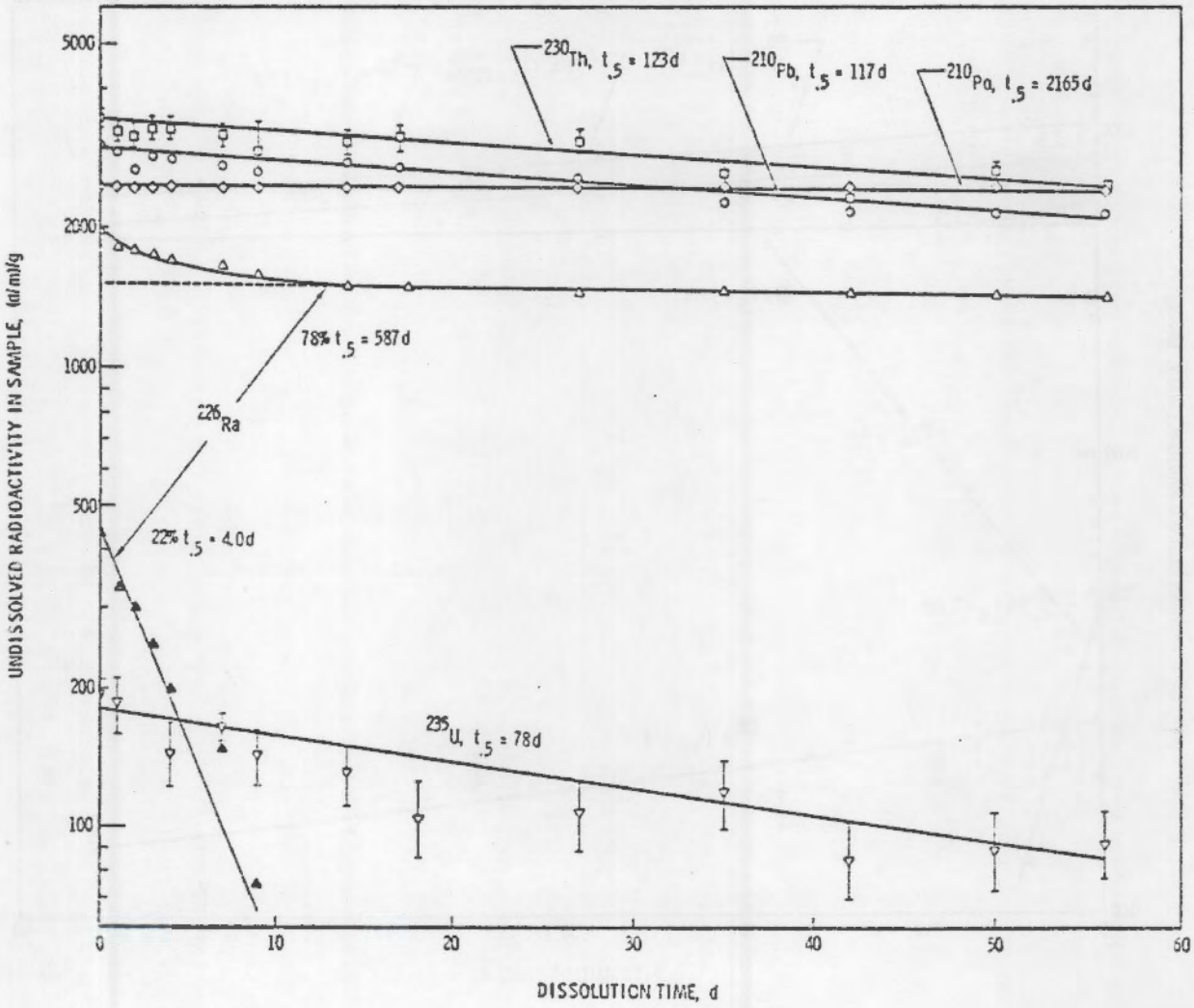

FIGURE 10. Dissolution of Airborne Ore-dust Sample A
Filled symbols indicate contributions of short-lived components.

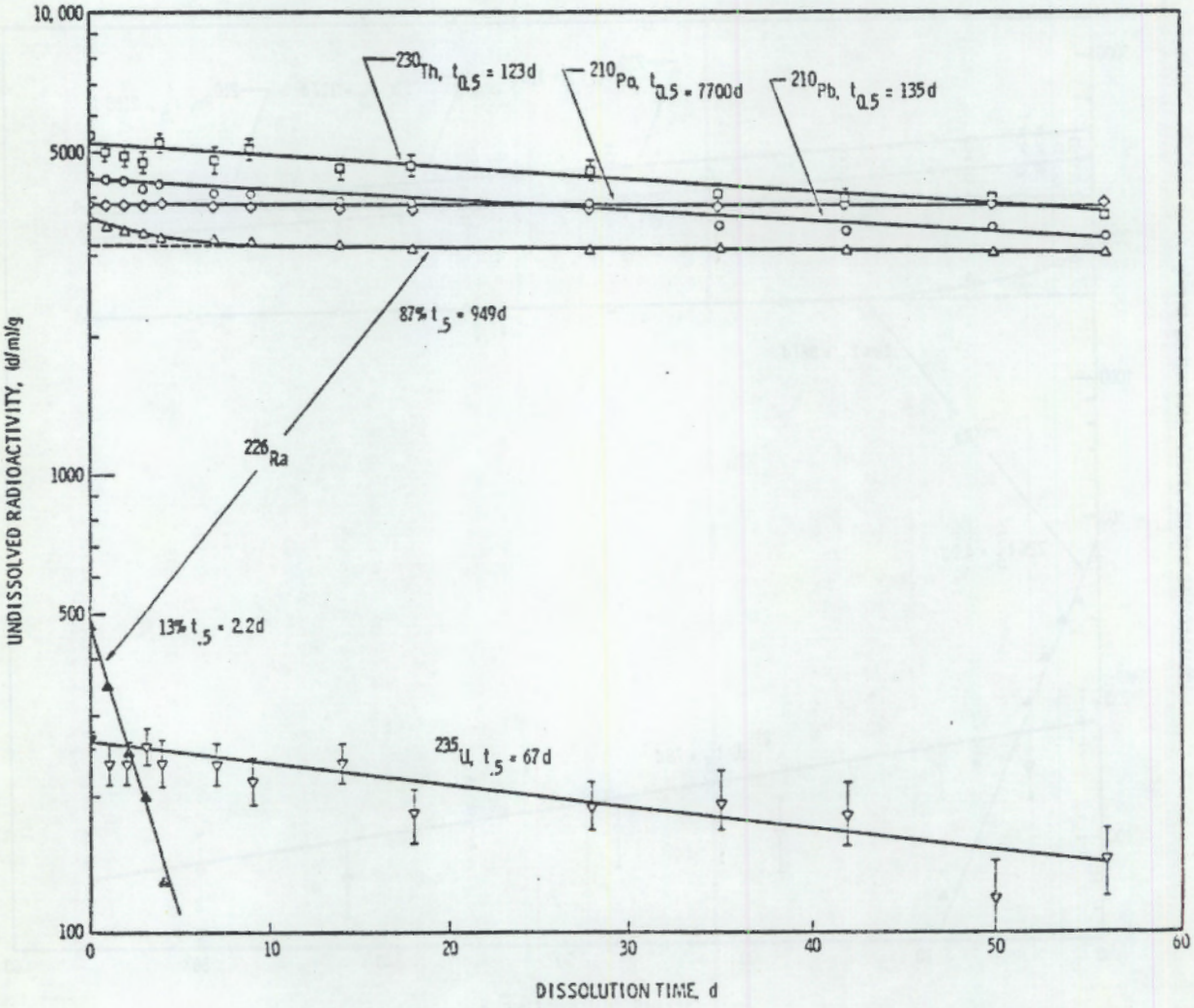

FIGURE 11. Dissolution of Airborne Ore-dust Sample B. Filled symbols indicate contributions of short-lived components.

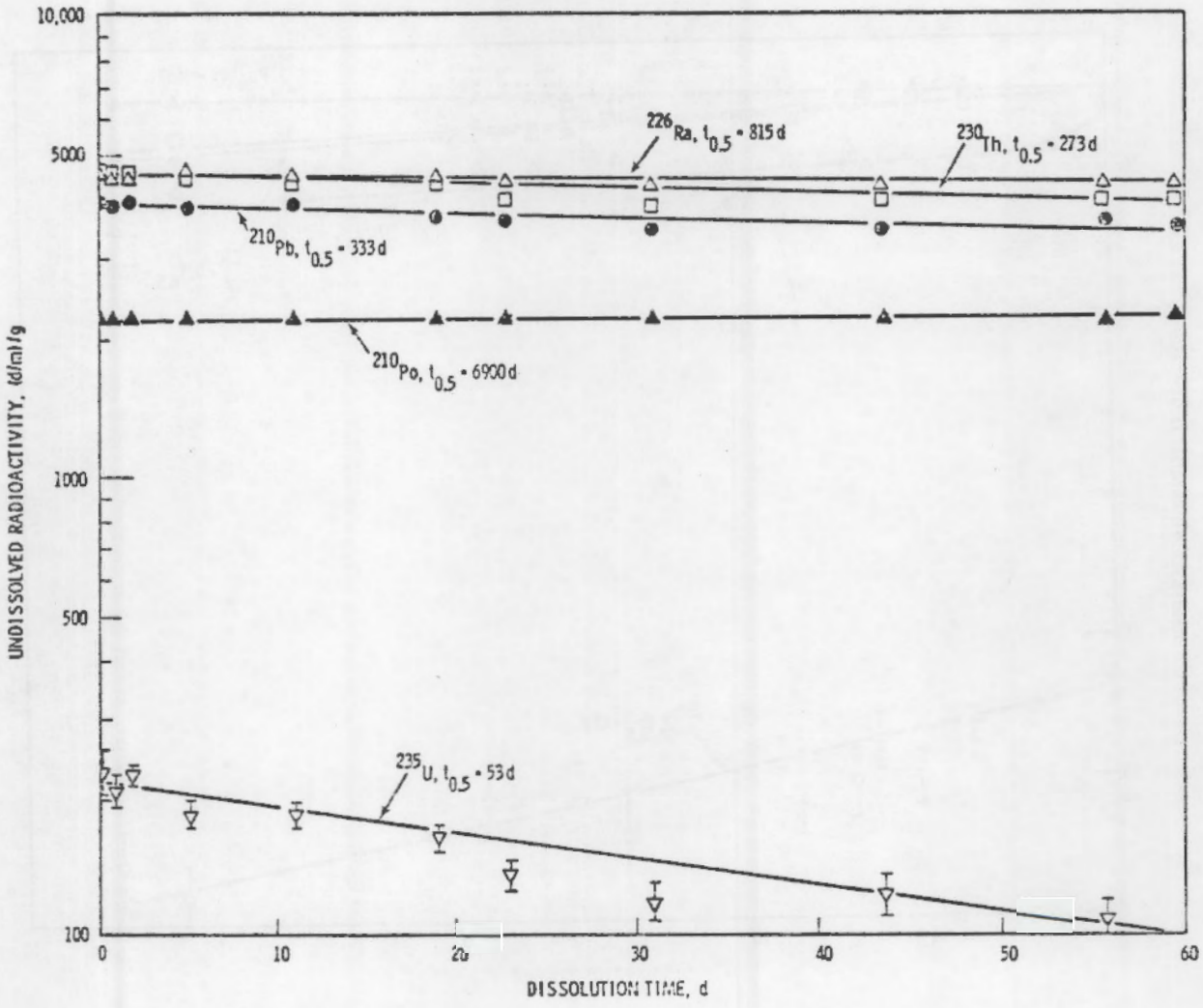

FIGURE 12. Dissolution of Airborne Ore-dust Sample C

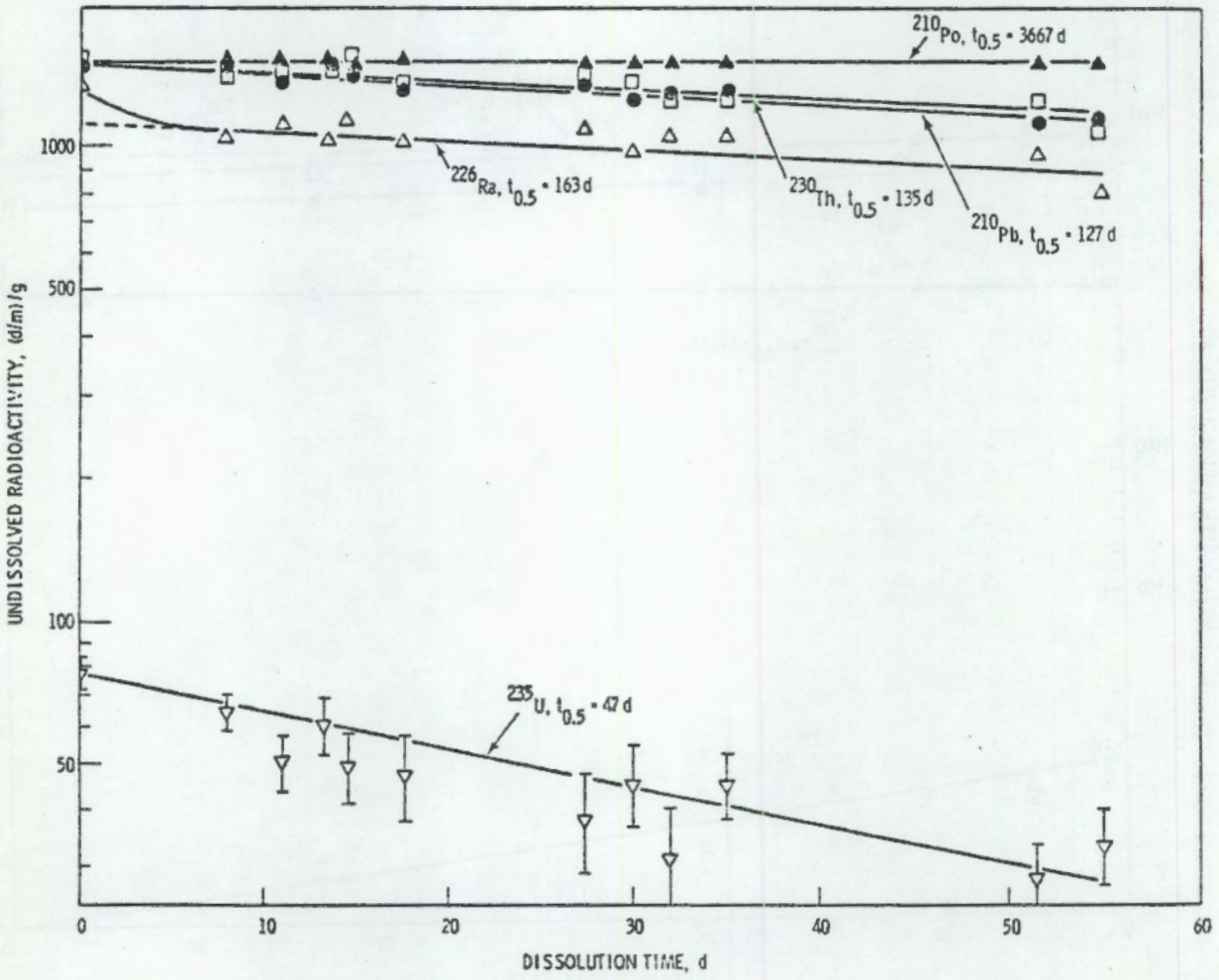

FIGURE 13. Dissolution of Ground-deposited Ore-dust Sample D

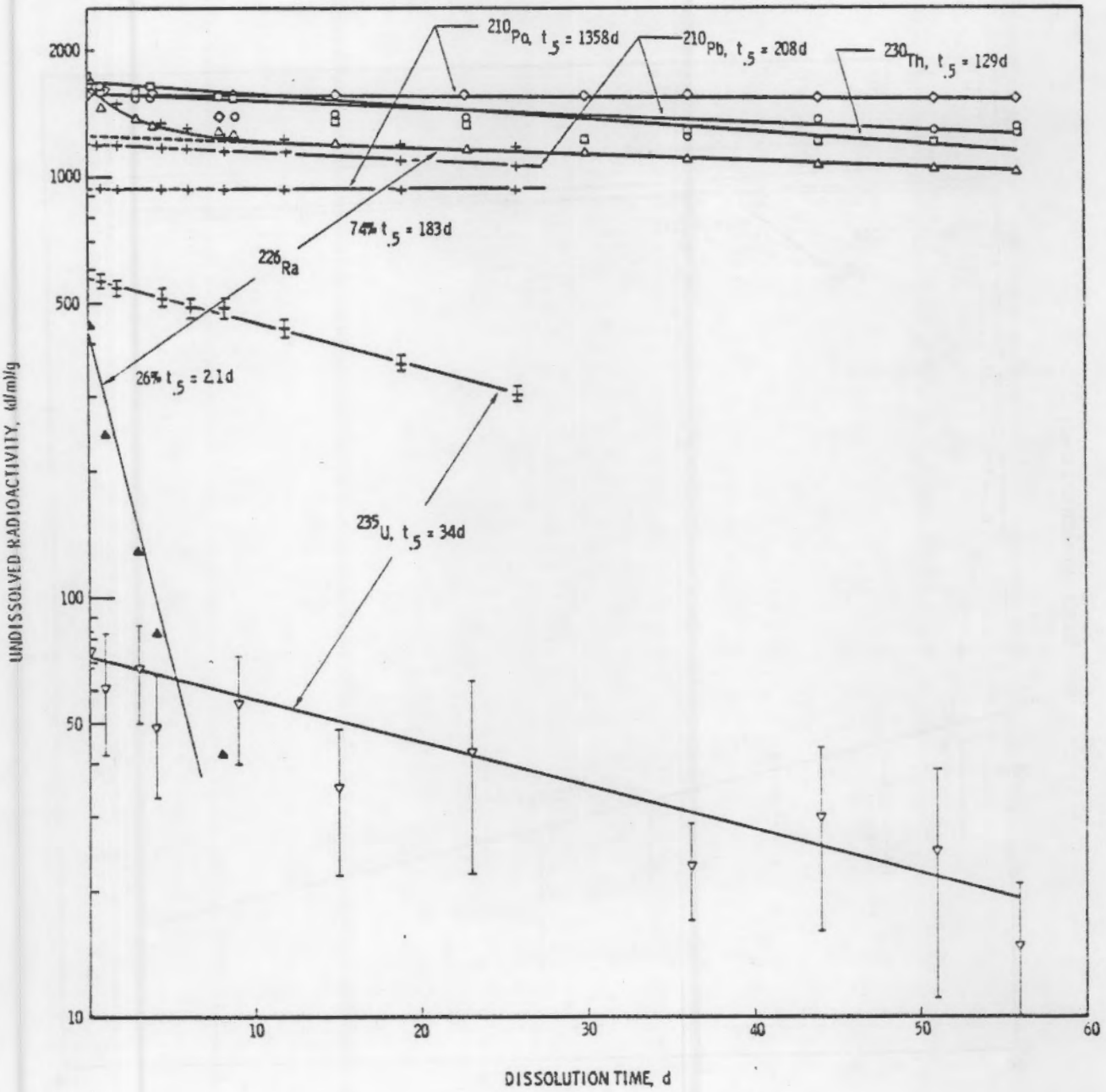

FIGURE 14. Dissolution of Ground-deposited Ore-dust Sample E. Filled symbols indicate contributions of short-lived components; crosses indicate dissolution of particles in the 1 to 7-μm size range.

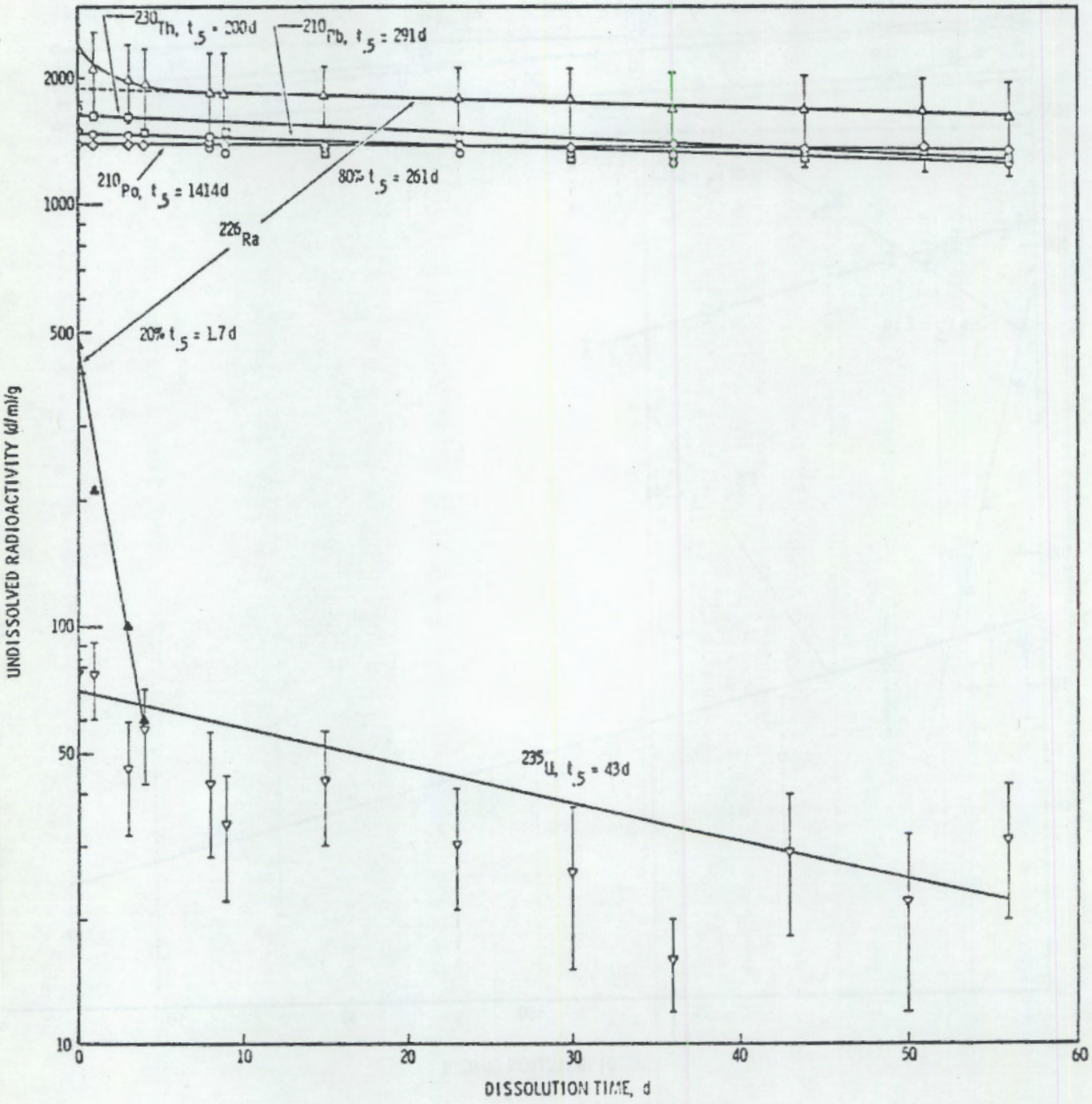

FIGURE 15. Dissolution of Ground-deposited Ore-dust Sample F. Filled symbols indicate contributions of short-lived components.

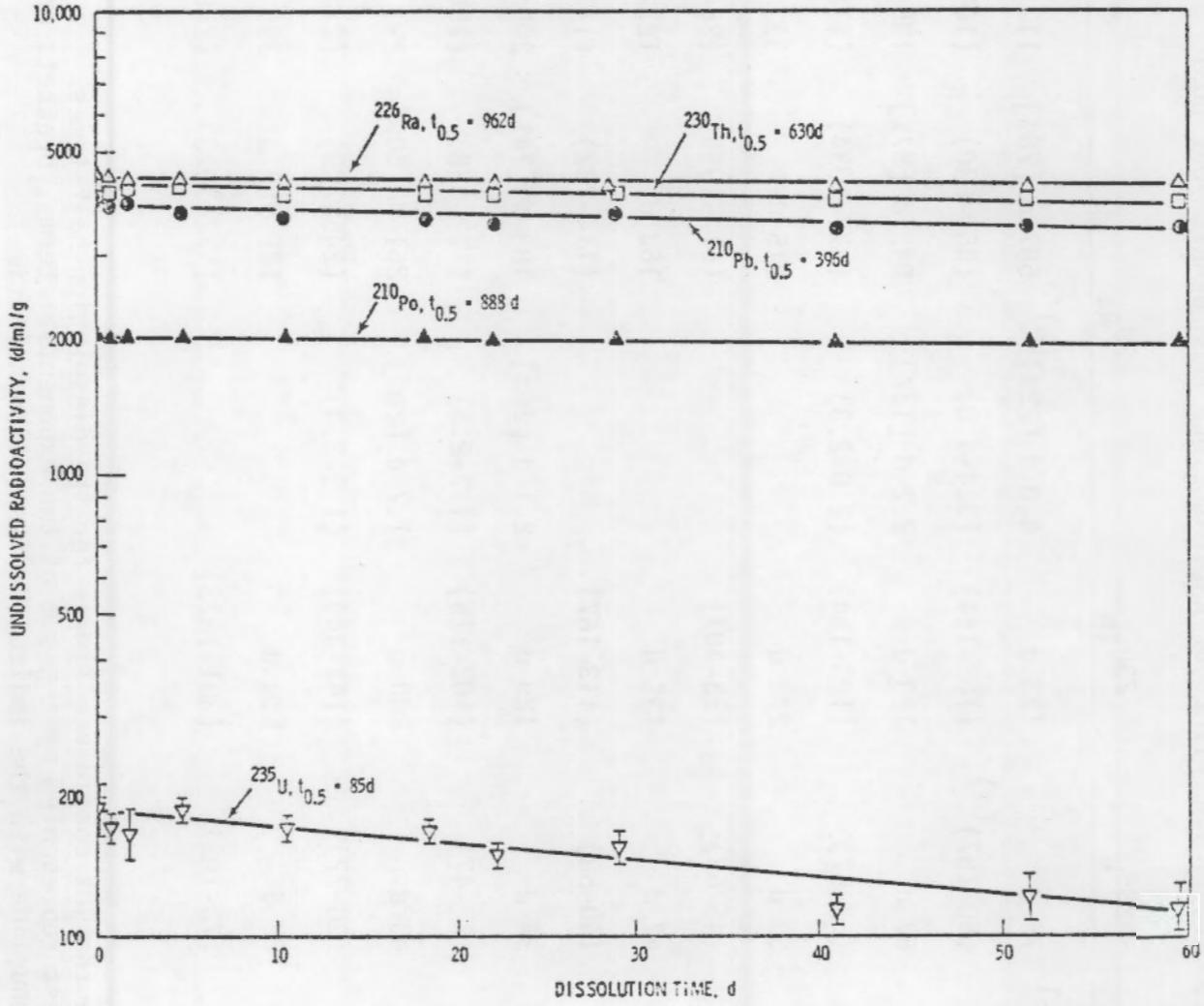

FIGURE 16. Dissolution of Ground-deposited Ore-dust Sample G

TABLE 7.
DISSOLUTION HALF-TIMES OF RADIONUCLIDES FROM URANIUM-ORE DUST

Sample	Type	Area	^{235}U	^{230}Th	^{226}Ra		^{210}Pb	^{210}Po
A	Airborne	5.0 m^2g^{-1}	78 d	123 d	4.0 d [22%][b]	587 d [78%]	117 d	2165 d
			(50-167)[a]	(102-154)	(3.4-4.8)	(550-630)	(101-182)	(1873-2567)
B	Airborne	5.2	67 d	123 d	2.2 d [13%]	949 d [87%]	135 d	7700 d
			(57-82)	(103-154)	(2.0-2.3)	(877-1034)	(118-158)	(4331-34,650)
C	Airborne	3.6	53 d	273 d		815 d	333 d	6930 d
			(46-63)	(83-407)		(517-1925)	(264-465)	(5775-8662)
D	Ground	3.1	47 d	135 d		163 d	127 d	3667 d
			(40-58)	(113-167)		(114-282)	(113-146)	(3209-8557)
E	Ground	3.3	34 d	129 d	2.1 d [26%]	183 d [74%]	208 d	1358 d
			(27-47)	(102-175)	(1.7-2.5)	(177-188)	(150-338)	(1194-1575)
F	Ground	4.5	43 d	200 d	1.7 d [20%]	261 d [80%]	291 d	1414 d
			(30-77)	(141-340)	(1.3-2.4)	(245-279)	(212-462)	(1260-1611)
G	Ground	4.1	85 d	630 d		TBE 962 d	396 d	888 d
			(72-103)	(381-1823)		(572-3013)	(286-641)	(825-962)

(a) Parentheses enclose the 90% confidence limits for the dissolution half-times.
(b) If the data were best represented by the sum of two exponential terms, brackets enclose the percentage of radionuclide with the indicated dissolution half-time.

both airborne samples and deposited samples had similar specific surface areas and thus, presumably, similar particle-size distributions.

A portion of sample E was fractionated according to particle size, and particles in the 1 to 7-μm range were dissolved separately. The results are plotted as crosses in Figure 14 and show that although the concentrations of uranium and its daughters were significantly greater in the finer particles, there was no difference between the dissolution behaviors of this fraction and the bulk sample.

Whereas the specific activities of ^{235}U, ^{230}Th, and ^{210}Pb in the undissolved dust were determined by direct gamma counting, those for ^{226}Ra and ^{210}Po had to be determined from the differences between their initial activities and the activities found in the liquid phase after filtration. Thus, it was important to ascertain the amounts of these radionuclides that might be adsorbed on the surfaces of the glass dissolution flasks. Fortunately, acid washes of the flask walls showed that negligible amounts of ^{226}Ra or ^{210}Po had adsorbed to the glass.

Possible readsorption of ^{210}Po on the undissolved particles was also investigated in order to better understand the slow dissolution of that radionuclide. It was tested indirectly by suspending a silver disc, which readily adsorbs polonium from solution, in the dissolving suspension and then counting the disc for ^{210}Po-alpha particles after a 1-week exposure. Negligible polonium was found on the disc, and it was concluded that the apparently slow dissolution of polonium from ore dust was due to its slow release from the particles rather than a rapid

release followed by readsorption at other sites on the particle surfaces.

DISSOLUTION OF RADIONUCLIDES FROM TAILINGS-PILE DUST

The dissolution rates of ^{230}Th, ^{226}Ra, ^{210}Pb, and ^{210}Po from nine samples of tailings-pile dust were evaluated. Uranium-235 was detected in a few samples at specific activities up to 10 (d/m)/g, but dissolution rates could not be evaluated starting with such low values. Six of the samples were collected directly on the tailings piles either as airborne dust or as surface deposits on the ground. Their dissolution patterns are shown in Figures 17 through 22. Generally, the specific activities of undissolved radionuclides decreased exponentially with time; but for several samples, the data for ^{226}Ra were better represented by the sum of two exponential terms. In one sample with extremely high specific surface area, even the data for ^{230}Th and ^{210}Pb were better represented by the sum of two exponential terms. Values for these parameters and the specific surface areas for the samples are listed in Table 8. Samples K and L were collected from the same location, but sample K contained all particles that passed through a sieve with 45-μm apertures, whereas sample L was a subfraction that passed through a sieve with 30-μm apertures. The specific surface area of sample L was found to be twice as large, but the effect on the dissolution half-times varied from nuclide to nuclide.

Three of the tailings-dust samples were collected at distances of 100 to 500 meters from the edges of the tailings piles

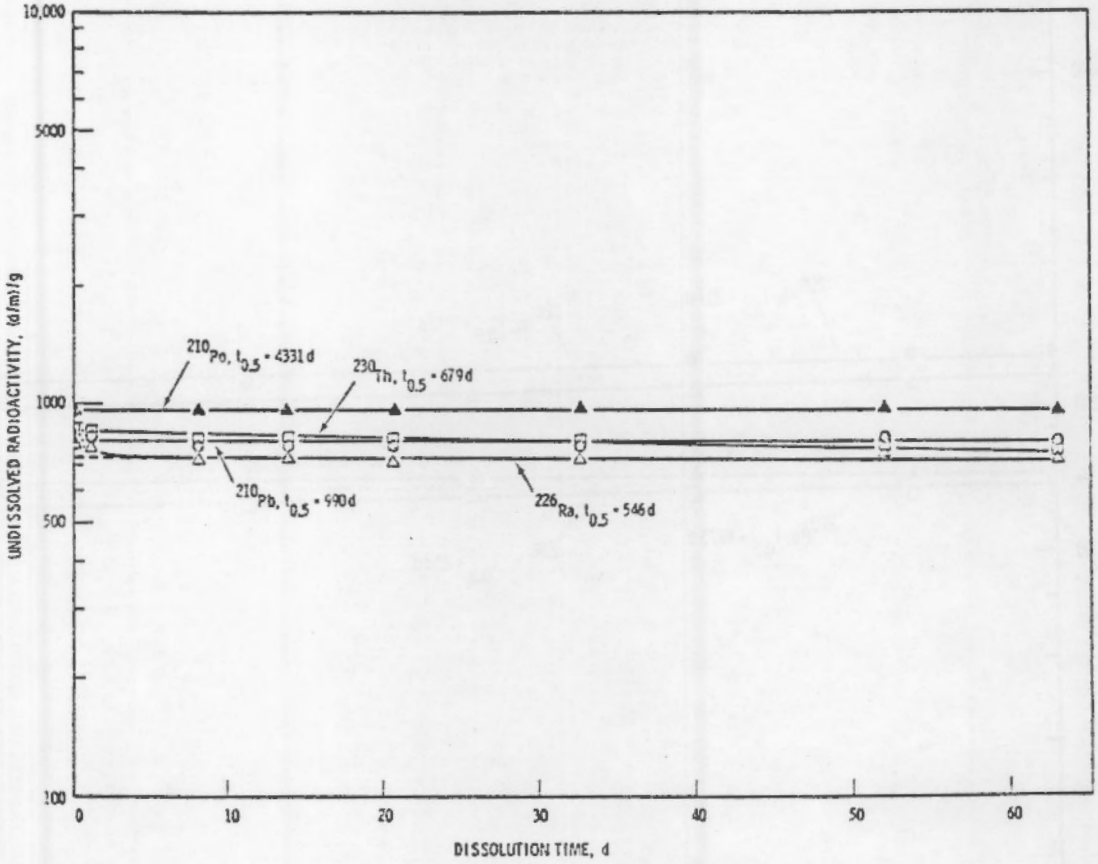

FIGURE 17. Dissolution of Airborne Tailings-dust Sample H

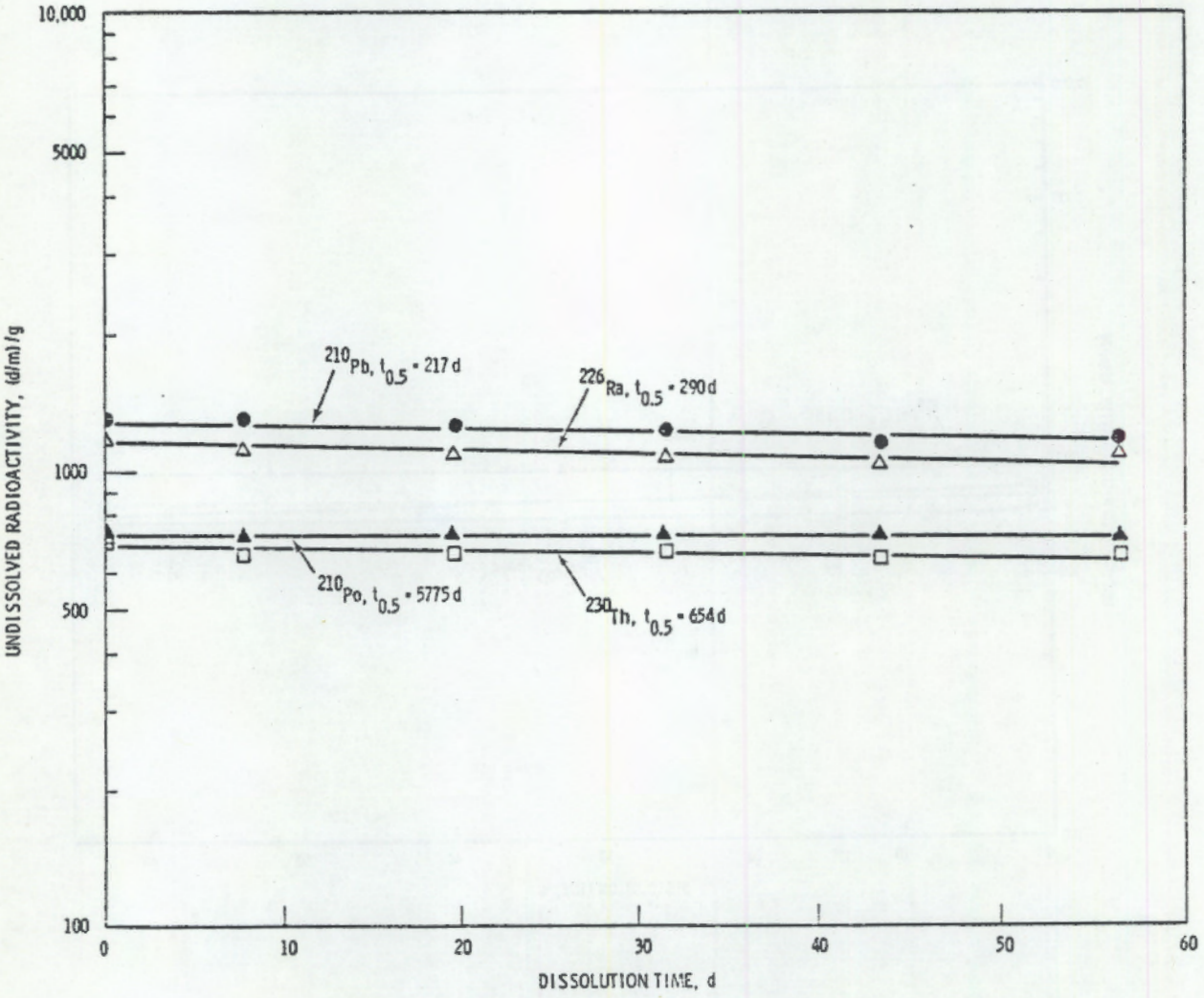

FIGURE 18. Dissolution of Airborne Tailings-dust Sample I

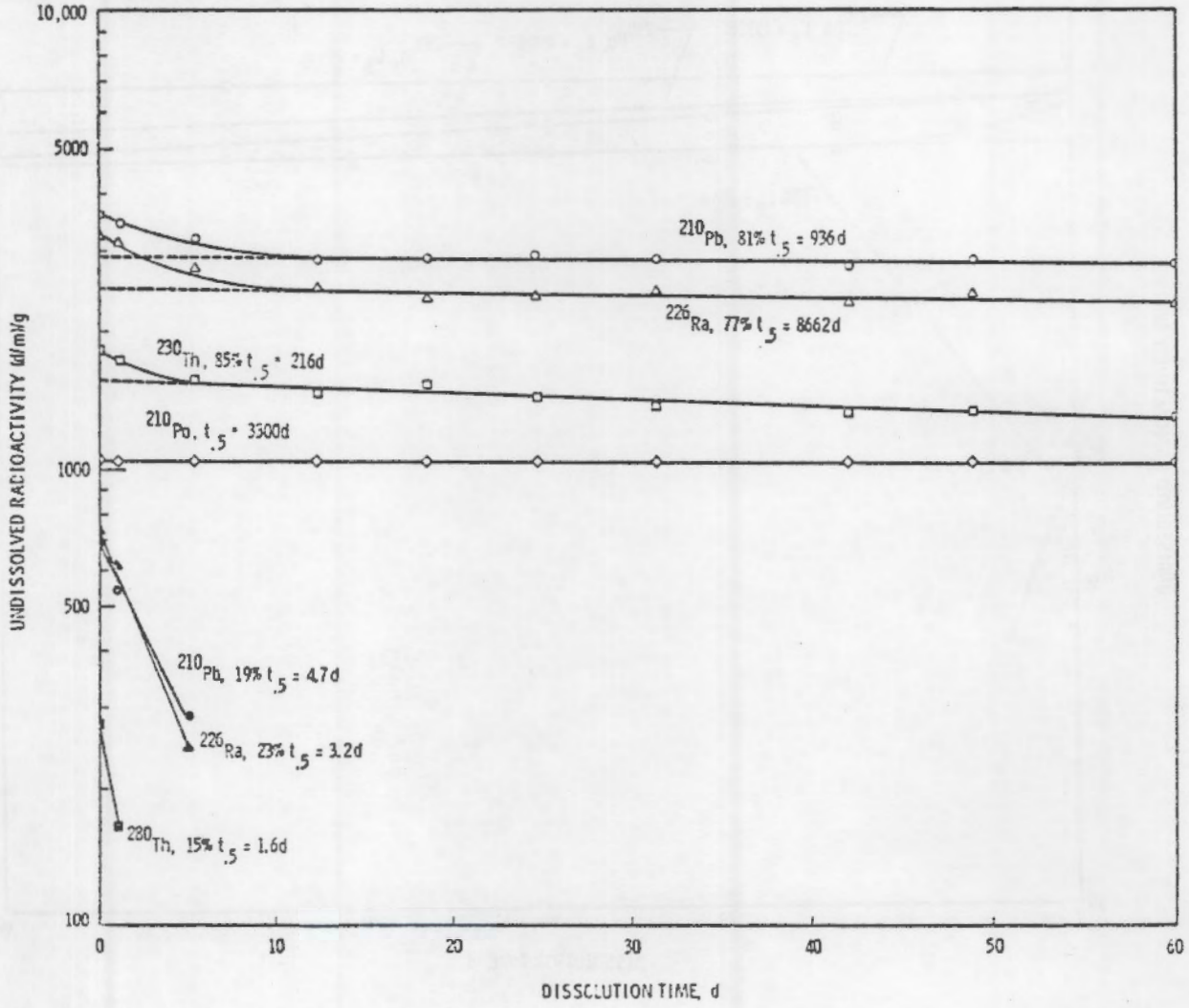

FIGURE 19. Dissolution of Ground-deposited Tailings-dust Sample J. Filled symbols indicate contributions of short-lived components.

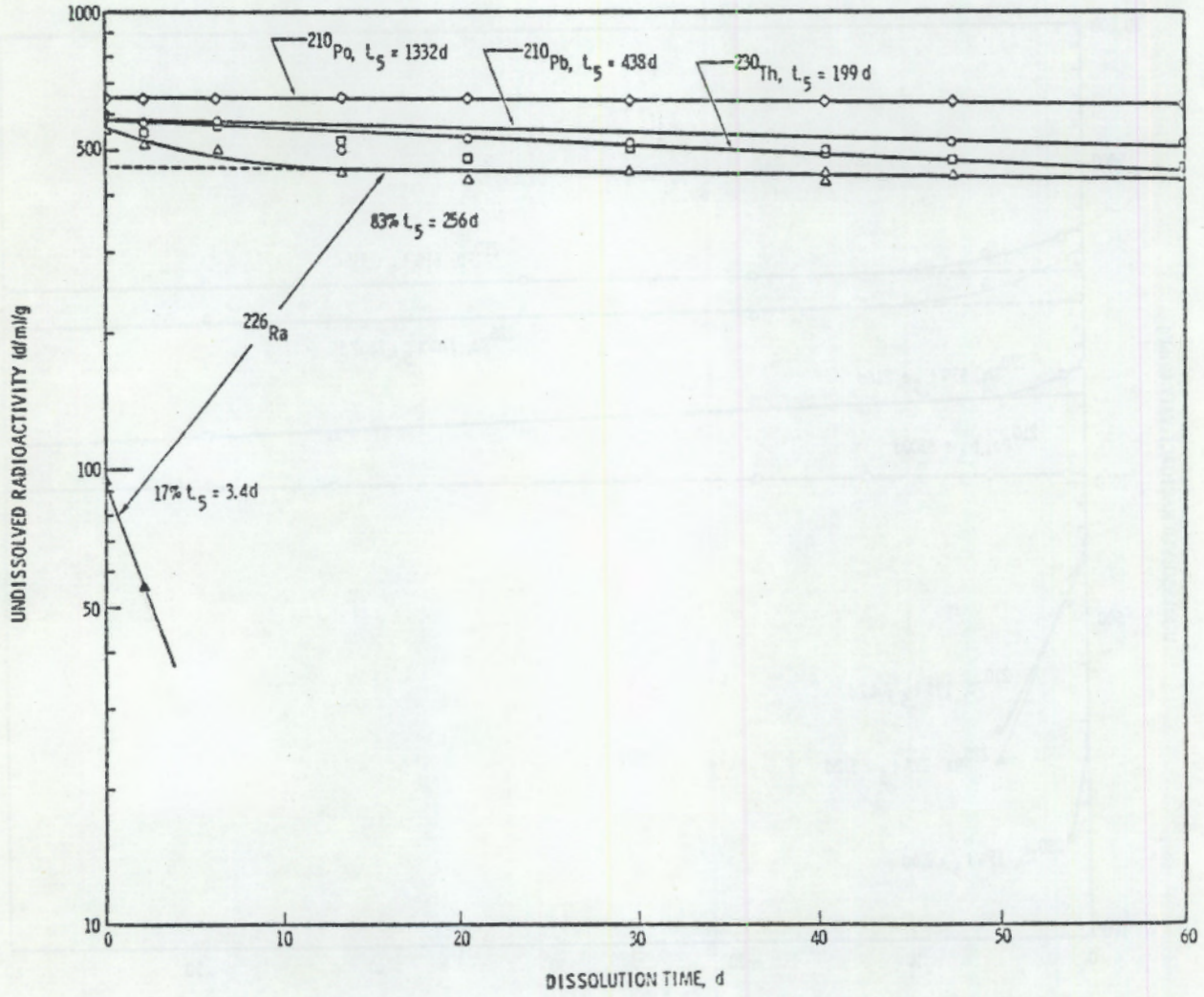

FIGURE 20. Dissolution of Ground-deposited Tailings-dust Sample K. Filled symbols indicate contributions of short-lived components.

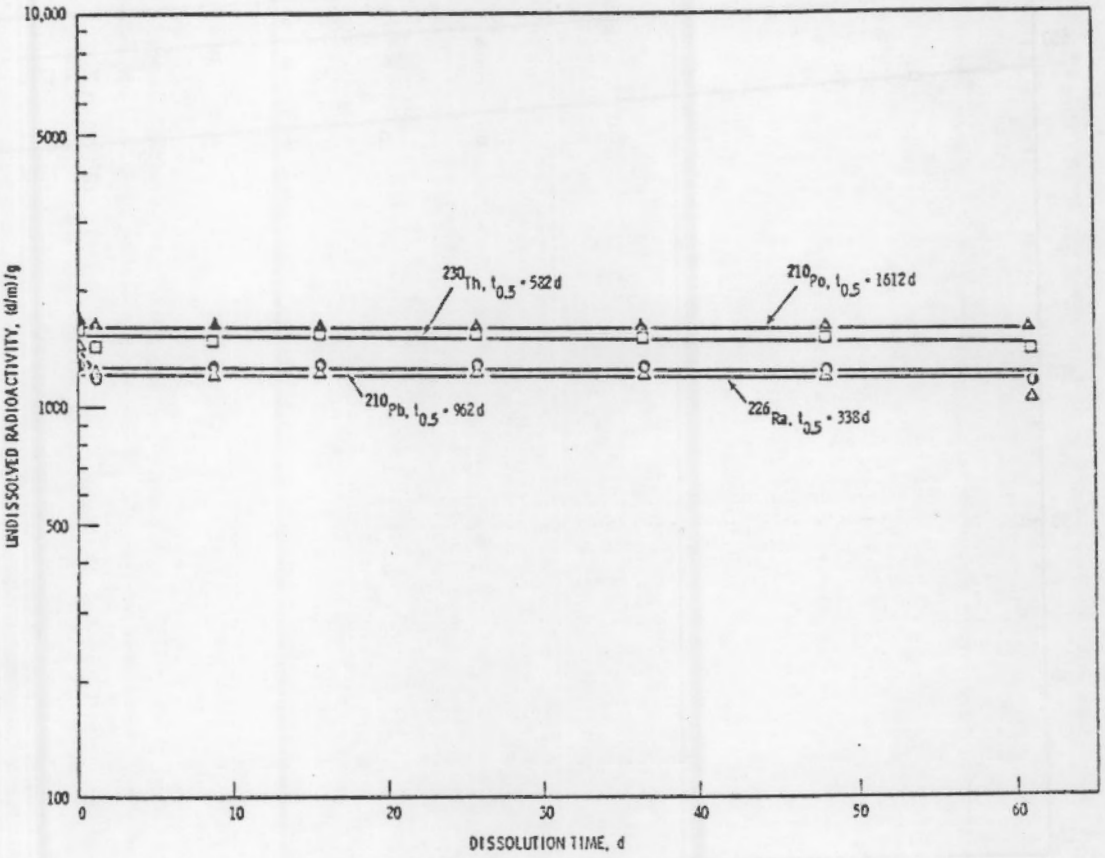

FIGURE 21. Dissolution of Ground-deposited Tailings-dust Sample L

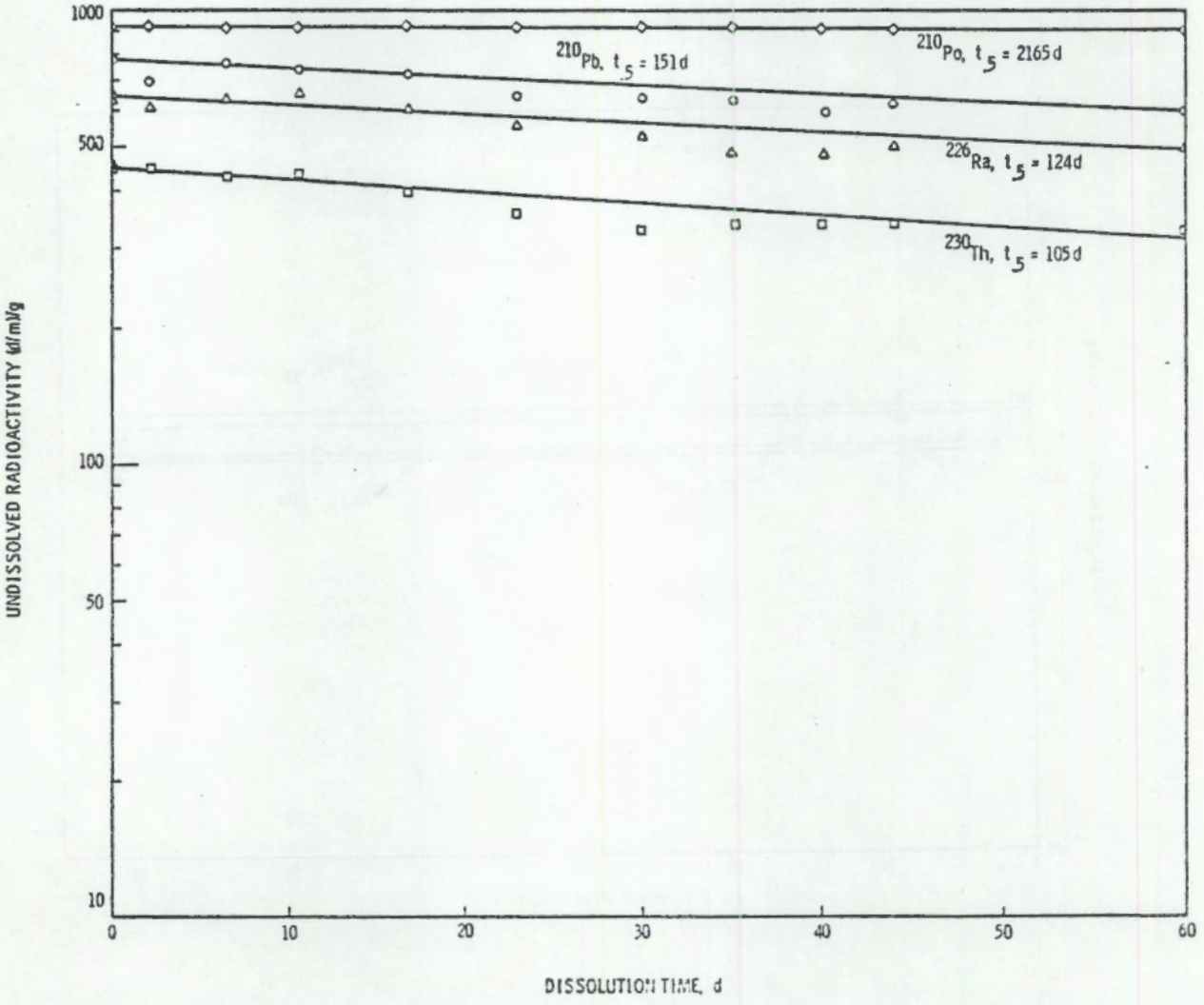

FIGURE 22. Dissolution of Ground-deposited Tailings Dust Sample M

FIGURE 8

DISSOLUTION HALF-TIMES OF RADIONUCLIOES FROM TAILINGS OUST COLLECTED ON VARIOUS PILES

Sample	Type	Area	^{230}Th	^{226}Ra	^{210}Pb	^{210}Po
H	Airborne (Mill 3)	3.1 m^2g^{-1}	679d (602-779)[a]	<1d[6%][b] 546d[95%] (481-630)	990d (855-1174)	4331d (4076-4620)
I	Airborne (Mill 4)	4.6	654d (495-962)	290d[100%] (217-433)	654d (495-962)	5775 (5331-6300)
J	Ground (Mill 1)	35.2	216d[95%][c] (187-312)	3.2d[23%] 1194d[77%] (1050-1386)	936d[81%][d] (636-1777)	3300d (3150-3465)
K	Ground (Mill 3)	4.3	199d (151-292)	3.4d[17%] 1386d[83%] (900-3013)	438d (254-1161)	1332d (1260-1414)
L	Ground (Mill	8.6	582d (412-990)	<1d[15%] 338d[85%] (174-5775)	926a (509-8662)	1612d (1474-1777)
M	Ground (Mill 4)	5.1	105d (91-125)	124d (105-150)	151d (124-191)	2165d (1872-2567)

(a) Parentheses enclose the 90% confidence limits for the dissolution half-times.

(b) If the data were best represented by the sum of two exponential terms, brackets enclose the percentage of radionuclide with the indicated dissolution rate.

(c) 15% of the ^{230}Th in this sample had a dissolution half-time of 1.6d.

(d) 19% of the ^{210}Pb in this sample had a dissolution half-time of 4.7d.

on roads that marked the general perimeter of the tailings-pile areas. All were samples of airborne dust, and their dissolution patterns are shown in Figures 23 through 25. Again, the specific activities of all radionuclides remaining undissolved decreased exponentially with time except for ^{226}Ra that required the sum of two exponential terms. Values for these parameters and the specific surface areas of the samples are listed in Table 9.

Tailings-pile samples H, K, L, and O were collected near a mill using the alkaline-leach process for uranium recovery, whereas the other samples were collected at mills using the acid-leach process. Despite this difference in source material, no significant difference was found in the dissolution rates of radionuclides from these two types of samples.

TABLE 9. Dissolution Half-Times of Radionuclides from Tailings Dust Collected at the Perimeters of Various Tailings-Pile Areas

Sample	Distance	Area	^{230}Th	^{226}Ra		^{210}Pb	^{210}Po
N	500 m (Mill 1)	31.7 m^2g^{-1}	70 d (58-202)	<1d[9%][b]	481d[91%] (320-1100)	396 d (264-788)	2310 d (1611-4076)
O	100 m (Mill 3)	1.6	447 d (357-597)	<1d[7%]	679d[93%] (441-1474)	537 d (330-924)	1873 d (1732-2038)
P	100 m (Mill 4)	5.0	398 d (223-1824)	<1d[4%]	554d[96%] (389-962)	488 d (280-1824)	304 d (271-344)

(a) Parentheses enclose the 90% confidence limits for the dissolution half-times.

(b) If the data are best represented by the sum of two exponential terms, brackets enclose the percentage of radionuclide with the indicated half-time.

DISSOLUTION OF URANIUM TETRAFLUORIDE

Dissolution rates for two samples of uranium tetrafluoride dust were measured. These were both mill products, but they were prepared by different procedures. As shown in Figure 26, dissolution of the Kerr-McGee product can be expressed as a single exponential term, whereas dissolution of the Allied Chemical product must be expressed as the sum of two exponential terms. Values for the dissolution parameters and for the specific surface areas of the samples are listed in Table 10.

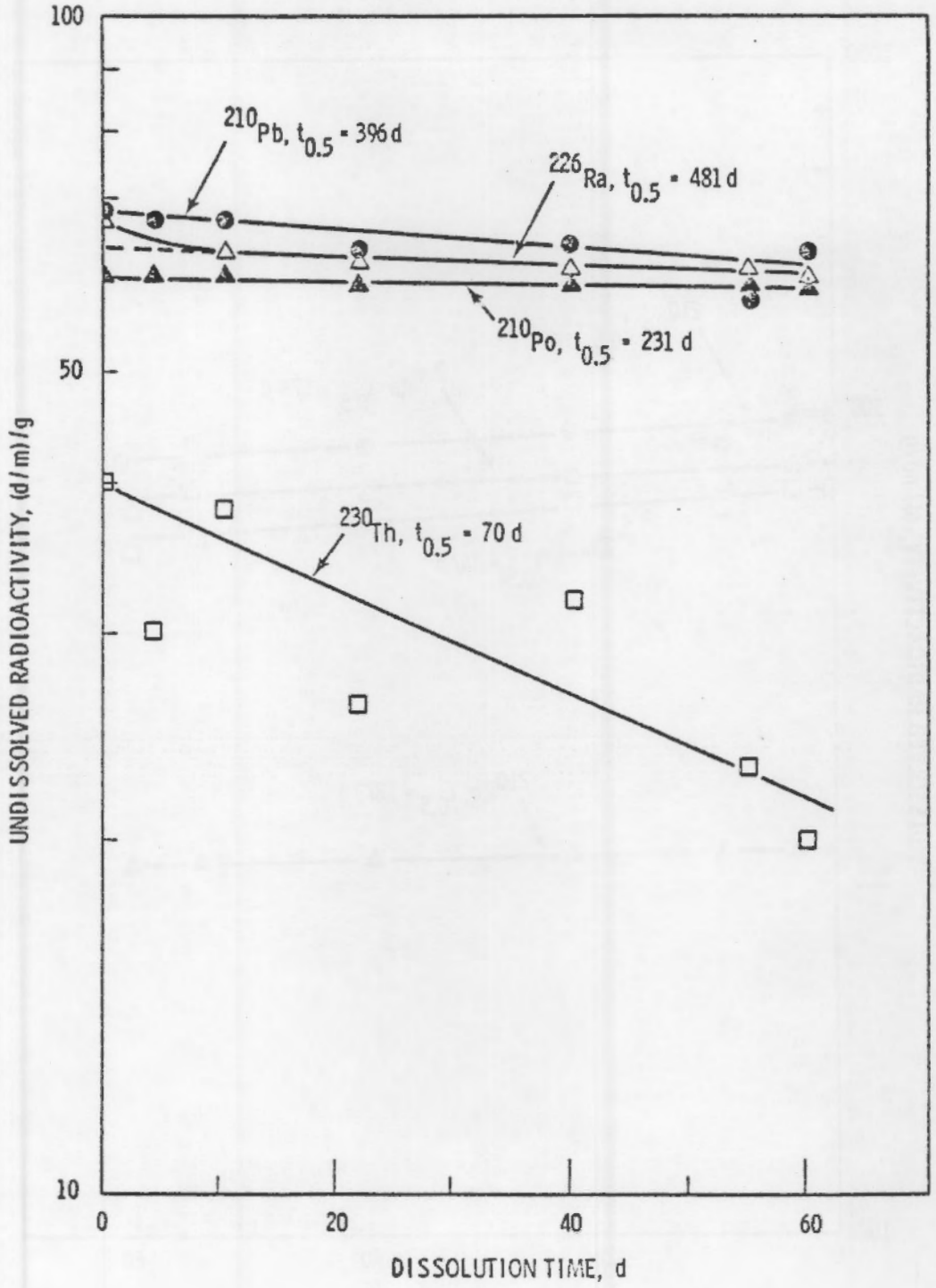

FIGURE 23. Dissolution of Airborne Perimeter-dust Sample N

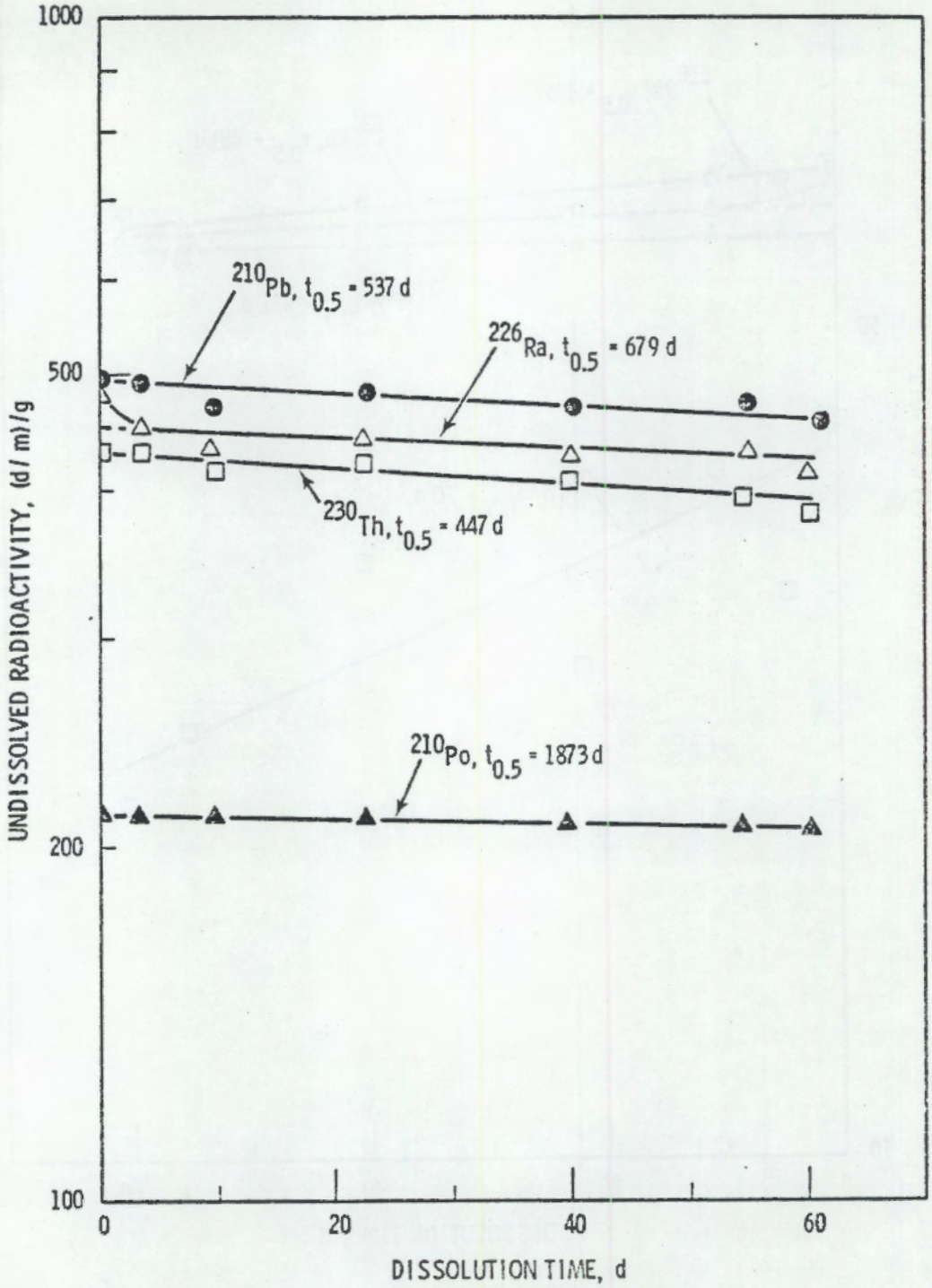

FIGURE 24. Dissolution of Airborne Permiter-dust Sample O

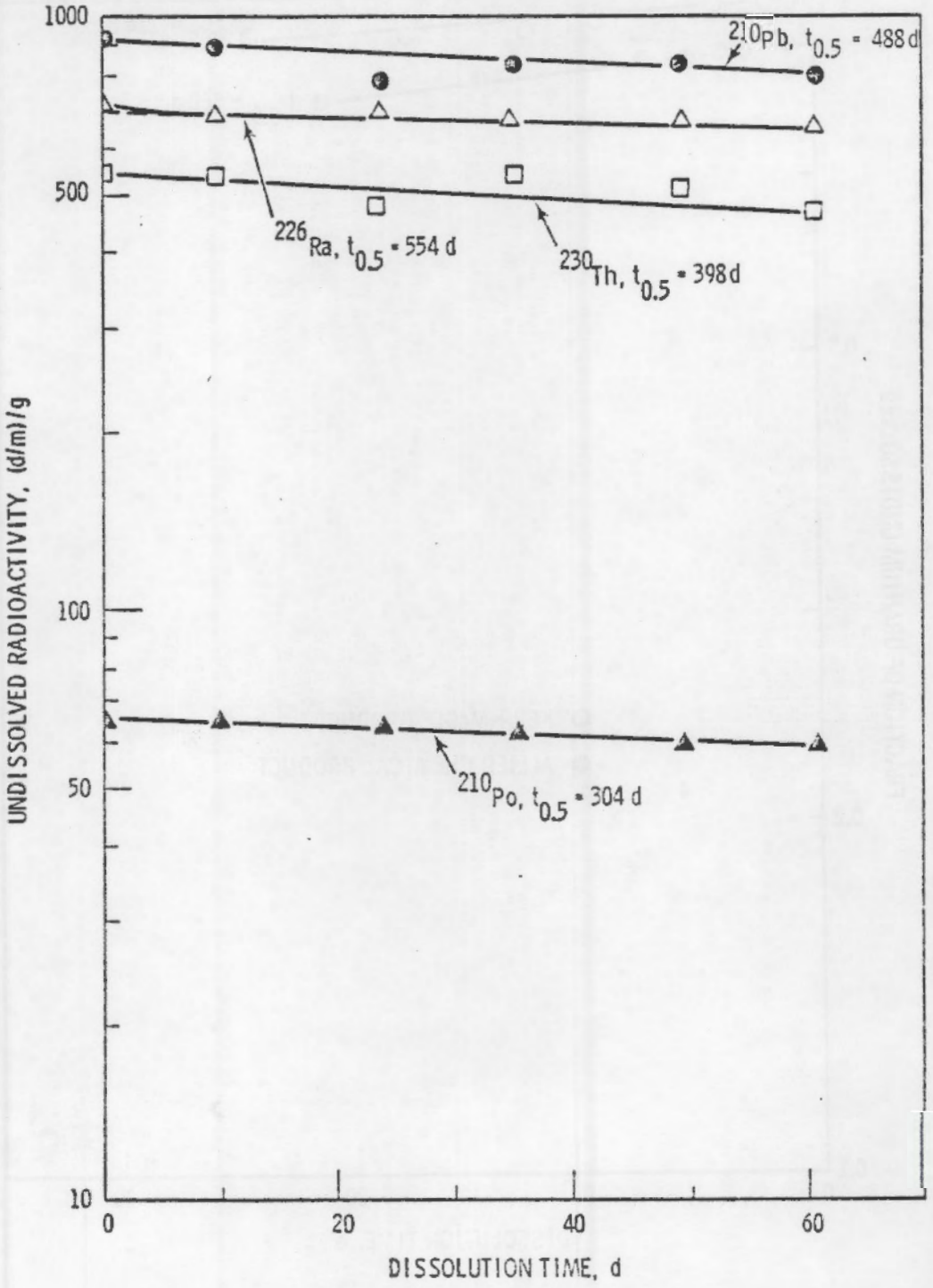

FIGURE 25. Dissolution of Airborne Perimeter-dust Sample P

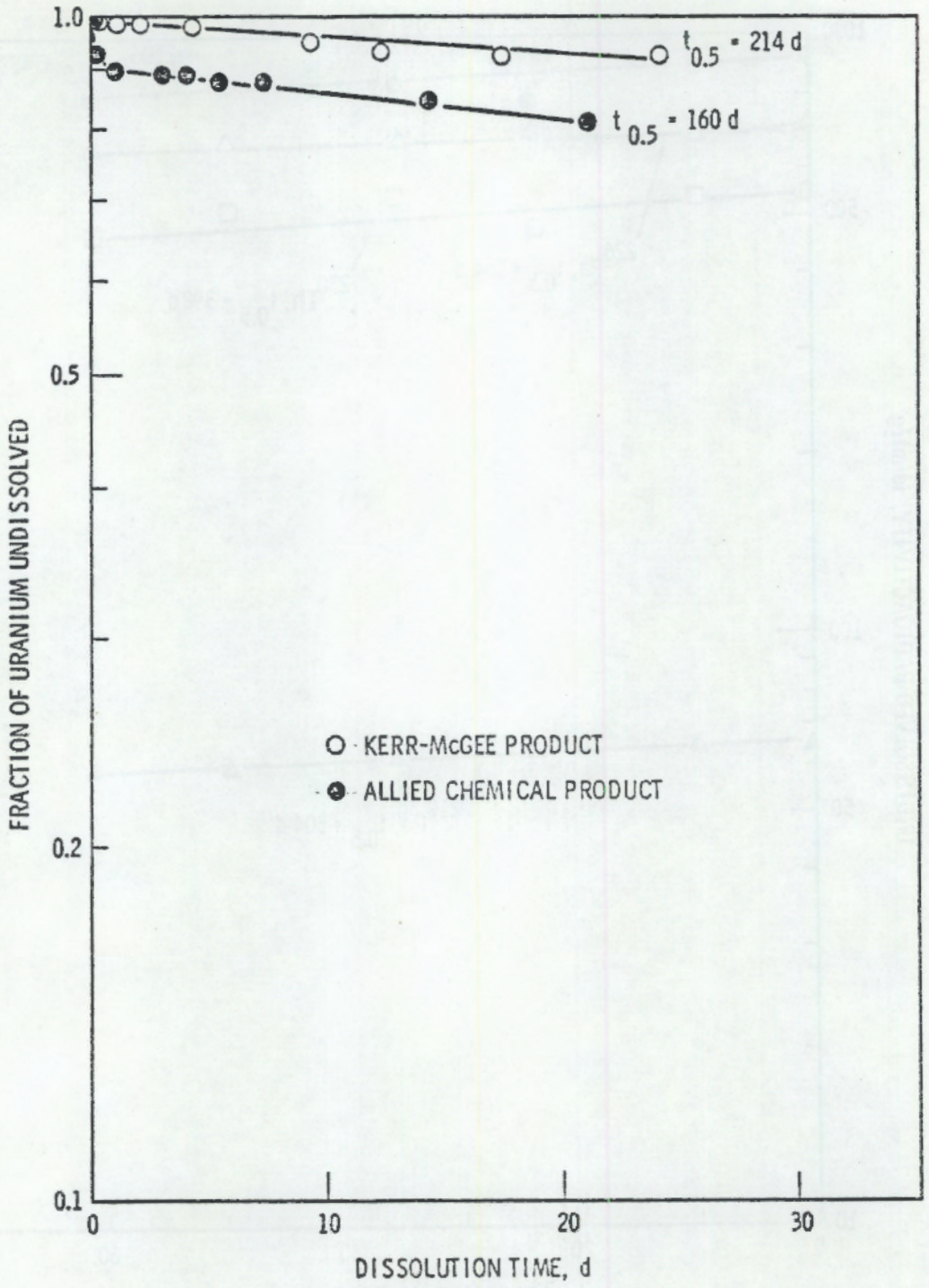

FIGURE 26. Dissolution of Uranium Tetrafluoride

The color of the Kerr-McGee product did not change during the dissolution process; but the Allied Chemical product, initially a mixture of green particles and a few gray particles, gradually turned into a mixture of black and yellow particles at the end of the 30-day examination.

TABLE 10. Physical Properties and Dissolution Parameters[a] of Uranium Tetrafluoride Samples

Producer	Area	Color	F_1	$(t_{0.5})_1$	F_2	$(t_{0.5})_2$
Kerr-McGee	0.3 m^2g^{-1}	Green	1.00	214 d (176-269)[b]		
Allied Chemical	1.6	Green + gray	0.90	160 d (144-178)	0.10	<0.1 d

[a] Values are given to express the fraction of undissolved uranium as, $F = F_1 \exp [-0.693t/(t_{0.5})_1] + F_2 \exp [-0.693t/(t_{0.5})_2]$.

[b] Parentheses enclose the 90% confidence limits for the dissolution half-times, $(t_{0.5})_i$.

DISCUSSION

INTERPRETATION OF THE DISSOLUTION PATTERNS

In this study, the fraction (or specific activity) of undissolved radionuclide in each sample was found to decrease with time either exponentially or in a biphasic pattern that could be described by the sum of two exponential terms. For pure compounds, theory[11] indicates that this decrease should be roughly exponential except for samples with very broad particle-size ranges; and an exponential decrease was indeed observed in the dissolution of ammonium diuranate, uranium oct-oxide, and one sample of uranium tetrafluoride. The specific

activities of ^{235}U, ^{230}Th, ^{210}Pb, and ^{210}Po in ore and tailings dust were also found to decrease exponentially during dissolution. Uranium dissolved fairly rapidly due to its reaction with carbonate ions in the simulated lung fluid to form the soluble $UO_2(CO_3)^{-4}$ ion. The other radionuclides do not form soluble carbonate complexes, and their dissolution half-times were found to be much longer.

Biphasic-dissolution patterns were observed for uranium from yellow-cake and the Allied Chemical samples of uranium tetrafluoride and for radium from ore and tailings dust. Three possible explanations were considered: [1] the radionuclides were initially present in two chemical forms, each with distinct dissolution half-times, [2] the samples had broad particle-size ranges, and [3] more slowly dissolving compounds of the radionuclides formed on the surface of the particles due to reaction with components in simulated lung fluid. The second possibility was ruled out for the yellow-cake samples since the same biphasic patterns were observed in the dissolution data from the fractions with narrow particle-size ranges. The third possibility was ruled out since the color stability of these samples indicated that no new compounds were formed at the surface. Therefore, it was concluded that the yellow-cake samples all contained uranium in two chemical forms but that the relative amounts in these forms varied from sample to sample.

The appearance of both gray and green particles in the uranium tetrafluoride from the Allied Chemical Co. strongly indicated that the biphasic dissolution pattern of this sample

was due to the presence of uranium in two chemical forms. The small amount of gray material could have easily accounted for the calculated amount of fast-dissolving uranium component. The subsequent color changes in the sample were undoubtedly due to reaction with components in simulated lung fluid, and the slow-dissolving uranium component was probably one of the reaction products.

The biphasic dissolution pattern of ^{226}Ra from ore and tailings dust was attributed to the gradual reaction of sulfate and carbonate ions from simulated lung fluid with a fast-dissolving radium compound on the surface of the parties. Any effect of particle-size range was ruled out since ^{226}Ra was the only component in these samples that showed the biphasic pattern.

COMPARISON OF AIRBORNE AND GROUND DUST

Both airborne and ground samples of uranium-ore dust, tailings-pile dust, and yellow-cake dust were examined, but no distinctive difference was observed between the specific surface areas of the two sample types. The range of values was wide, but generally, specific surface areas for some ground samples were higher than those for some airborne samples and vice versa. The only significant difference in dissolution behavior was seen among the samples of yellow-cake dust. The entire airborne yellow-cake sample followed a dissolution half-time of less than 10 days whereas the ground samples had significant amounts of slower dissolving material. Even here,

however, this difference may have been due to the dissimilarity of the sampling locations. The airborne dust was collected at a vent near the start of the drying operation whereas the ground samples were all collected at the final stage of their drying treatment. It is probable that the composition of yellow cake changes during drying to compounds that dissolve more slowly. Since there was no clear distinction between the properties of airborne and ground samples, data from both were pooled in determining the appropriate solubility classification for the radionuclides in a product.

EFFECT OF SPECIFIC SURFACE AREA AND PARTICLE SIZE

The dissolution half-time of a pure substance is expected to be inversely proportional to its specific surface area[10]. In the present study, this relationship was confirmed by the data for pure ammonium diuranate and the rapidly dissolving component in yellow cake which was assumed to be ammonium diuranate. The relationship was tested by examining whether the product of a sample's specific surface area and the dissolution half-time for its fast-dissolving component was a constant. From the 10 data pairs available, the 90% confidence interval for this constant was found to be 6 ± 2 $m^2 g^{-1} d$. Chemical heterogeneity probably obscured this relationship in samples of the other products.

The deposition of dust in the lungs is expected to be a strong function of particle size so that it was important to compare the dissolution rates of representative dust samples with those of their efficiently deposited size fractions. The

latter are generally thought to include particles in the 0 to 10-μm size range. Data on the yellow-cake dust from Mill 4 showed that particles in the 1 to 3-μm fraction dissolved at the same rate as the total sample, as would be expected from the similarities in their specific surface areas. Indeed, the specific surface areas of the dust fractions increased relatively slowly with decreasing particle size indicating the particles were very irregular in shape. Similarly, data on sample E of uranium ore dust showed that the radionuclides in the 1 to 7-μm fraction exhibited the same dissolution patterns as the total sample. Again, this would be consistent with a collection of irregularly shaped particles whose specific surface area increased only gradually with decreasing particle size but which contained radionuclides in a rather homogeneous matrix.

SOLUBILITY CLASSIFICATION OF PRODUCTS

The solubility classifications of products were based directly on their dissolution half-times in simulated lung fluid at 37°C. If the product contained radionuclides that dissolved at different rates, a composite classification was assigned to show the solubility classifications for the components. If a radionuclide appeared to be present in two chemical forms that dissolved at significantly different rates, a mixed classification was assigned to show the percentage of radionuclide in each solubility class.

Uranium Octoxide

The results of this study indicate that uranium octoxide should be assigned the solubility classification Y. Five

samples were examined, and in each case, over 90% of the uranium dissolved very slowly with a dissolution half-time greater than 100 days. A rapidly dissolving component was detected in all samples, but since it accounted for less than 10% of the uranium, it was neglected. The Y classification confirms that recommended for uranium octoxide by Steckel and West[2] and by Cooke and Holt[3].

Ammonium Diuranate

The dissolution half-time of ammonium diuranate was found to be 0.2 to 0.3 days, placing it in solubility class D. Cooke and Holt[3] assigned this compound the solubility classification W based on the dissolution behavior of their samples. This discrepancy is probably due to differences between the chemical compositions of the products examined in the two studies. Cooke and Holt did not report the chemical composition of their sample, but it may have contained thermal decomposition products of ammonium diuranate, formed during drying, that dissolved more slowly. It seems unlikely that the slower dissolution rate they found was due to a lower specific surface area since the particles in their sample were considerably smaller than those used in the present study.

Yellow-Cake Dust

Classification of yellow cake poses a special problem since the term "yellow cake" covers a variety of materials with different color, chemical composition, and dissolution behavior. Ammonium diuranate, a bright yellow compound, is generally the target product in yellow-cake production; but during the drying

operation, the color and chemical structure of the actual product gradually changes due to thermal decomposition. At the two extremes of the heating process are ammonium diuranate in solubility class D and uranium octoxide in solubility class Y. Thus it is not surprising that both fast- and slow-dissolving components were detected in most of the samples examined, and their relative amounts were quite different. Independent dissolution-rate determinations on four of the same yellow-cake samples by Eidson and Mewhinney[12] confirmed this behavior. A comparison of the solubility classifications that were derived from the two investigations is shown in Table 11. Good agreement was found in the relative amounts,

TABLE 11. Comparison of Solubility Classifications for Yellow Cake

Sample	Edison and Mewhinney[12]	This Work
Mill 1	78% D, 22% Y	78% D, 22% W
Mill 2	26% D, 74% Y	36% D, 64% Y
Mill 3	61% D, 39% Y	50% D, 50% W
Mill 4	64% D, 20% Y	61% D, 39% W
Mill 4 (Airborne)		100% D

and dissolution half-times of the fast-dissolving components in each sample, and Eidson and Mewhinney also reported X-ray powder diffraction patterns supporting the view that ammonium diuranate was present in each of the samples. The dissolution half-times of the slow-dissolving components were found to be shorter in the present study, putting three of them in class W. This difference may be due to the lower pH used in the present work, 7.3 vs. 7.6, and the absence of any DTPA chelating agent or antibacterial agent as used by the other investigators.

The average amount of the fast-dissolving component in the five samples was 60% so that a mixed classification of 60% D - 40% W generally describes their composite dissolution behavior. The classification W was chosen for the slow-dissolving component because it is a conservative compromise between the classifications for this component in the individual samples, assuming the main hazard of inhaled yellow cake is kidney damage. Judging from the examples tested, individual samples of yellow cake may deviate significantly from the 60% D, 40% W classification, and dissolution half-times of particular products should be used for hazard evaluation when available.

Uranium-Ore Dust

The results of this study show that ^{230}Th, ^{210}Pb, and ^{210}Po in uranium-ore dust should be assigned the solubility classification Y since their dissolution half-times from all samples were greater than 100 days. Uranium (^{235}U,^{238}U) exhibited dissolution half-times ranging from 34 to 85 days and should, thus, be assigned the classification W. Radium-226 exhibited a biphasic dissolution pattern in four of the seven samples suggesting the presence of two chemical forms of radium. Considering the relative amounts of these forms indicated by the dissolution data, ^{226}Ra should be assigned the mixed classification 10% D, 90% Y.

Tailings-Pile Dust

As in the case of uranium-ore dust, ^{230}Th, ^{210}Pb, and ^{210}Po in tailings-pile dust should be assigned the classification Y. In two samples, ^{210}Pb and/or ^{230}Th dissolved initially with

shorter half-times, but these minor discrepancies were not considered to be characteristic of tailings-pile dust. On the other hand, ^{226}Ra exhibited a biphasic dissolution pattern in most of the samples and should be assigned the mixed classification 10% D, 90% Y. Although the specific activity of radionuclides in tailings-pile dust decreased with distance from the piles, as expected, the solubility classifications were not altered.

Uranium Tetrafluoride

The results of this study show that uranium tetrafluoride should be assigned the solubility classification Y since 90% or more of both samples had dissolution half-times in excess of 100 days. The fast-dissolving component in the Allied Chemical product is probably a different compound of uranium, but it comprised only 10% of the total uranium in the sample. Both Steckel and West[2] and Cooke and Holt[3] also recommended that uranium tetrafluoride be assigned the solubility classification Y.

USE OF COMPOSITE AND MIXED SOLUBILITY CLASSIFICATIONS

Both composite and mixed solubility classifications are compatible with the ICRP Task Group Model for retention of radionuclides in the lung. A composite classification merely summarizes the solubility classifications of the component radionuclides and a mixed classification merely summarizes the solubility classification of a particular radionuclide. Thus, in the case of uranium-ore dust, a composite classification of (^{235}U,^{238}U) - W; (^{226}Ra) - 10% D, 90% Y; (^{230}Th,^{210}Pb,^{210}Po) - Y indicates that in the calculations of radionuclide retention and radiation dose,

all the deposited ^{235}U and ^{238}U should be assigned the inter-compartmental transfer parameters tabulated for class W compounds[13], all of the deposited ^{230}Th, ^{210}Pb, and ^{210}Po, as well as 90% of the ^{226}Ra, should be assigned the corresponding parameters for class Y compounds, and 10% of the deposited ^{226}Ra should be assigned the parameters for class D compounds.

REFERENCES

1. P. E. Morrow, T. T. Mercer, T. F. Hatch, B. R. Fish, and D. V. Bates, "Deposition and Retention Models for Internal Dosimetry of the Human Respiratory Tract." Health Phys. 12: 173-206, 1966.

2. L. M. Steckel and C. M. West, "Characterization of Y-12 Uranium Process Materials Correlated with In Vivo Experience." Y-1544A, Union Carbide Corporation, Oak Ridge Y-12 Plant, Oak Ridge, TN 37831, 1966.

3. N. Cooke and F. B. Holt, "The Solubility of Some Uranium Compounds in Simulated Lung Fluid." Health Phys. 27: 69-77, 1974.

4. P. E. Morrow, F. R. Gibb, and L. Johnson, "Clearance of Insoluble Dust from the Lower Respiratory Tract." Health Phys. 10: 543-555, 1964.

5. P. E. Morrow, F. R. Gibb, H. Davis, and M. Fisher, "Dust Removal from the Lung Parenchyma: An Investigation of Clearance Stimulants." Tox. and Appl. Pharm. 12: 372-396, 1968.

6. G. A. Sehmel, "Airborne Particulate Concentrations and Fluxes at an Active Uranium Mill Tailings Site." NUREG/CR-0258, Proceedings of the Seminar on Management, Stabilization, and Environmental Impact of Uranium Mill Tailings, Albuquerque, NM, 1978.

7. T. Allen, Particle Size Measurement, Second Edition, John Wiley and Sons, New York, NY, pp. 355-376, 1975.

8. O. R. Moss, "Simulants of Lung Interstitial Fluids," accepted for publication in Health Physics.

9. K. Diem and C. Lentner, ed., Documenta Geigy Scientific Tables, Seventh Edition. CIBA-GEIGY, Ltd., Basel, p. 523, 1970.

10. E. A. Moelwyn-Hughes, Physical Chemistry, Second Edition. Pergammon Press, New York, pp. 1215-1216, 1961.

11. T. T. Mercer, "On the Role of Particle Size in the Dissolution of Lung Burdens." Health Phys. 13: 1211-1221, 1967.

12. A. F. Eidson and J. A. Mewhinney, "In Vitro Dissolution of Uranium Product Samples from Four Uranium Mills." NUREG/CR-0414, LF 59, Lovelace Biomedical and Environmental Research Institute, Albuquerque, NM, 1978.

13. These values are listed in Table 4 of Reference 1.

ACKNOWLEDGMENTS

The assistance of several Battelle staff members is gratefully acknowledged: P. O. Jackson and C. W. Thomas - sample collection; O. R. Moss - recipe for simulated lung fluid and design of the pass-by dissolution chamber; C. Veverka and J. C. Langford - radiochemical analyses; and A. J. Roese, Battelle Columbus Laboratories - particle sizing. The assistance of the Hanford Engineering Development Laboratory, Westinghouse Electric Corporation, in determining specific surface areas of samples was also greatly appreciated.

DISTRIBUTION

No. of Copies

OFFSITE

A. A. Churm
DOE Patent Division
9800 S. Cass Avenue
Argonne, IL 60439

113 U.S. Nuclear Regulatory Commission
Division of Technical Information and Document Control
7920 Norfolk Avenue
Bethesda, MD 20014

2 DOE Technical Information Center
Washington, D.C. 20545

30 Dr. Lewis Battist
U.S. Nuclear Regulatory Commission
Environmental Protection Standards Branch
Office of Standards Development
Washington, D.C. 20555

Mr. William E. Gray
Manager
Environmental Engineering
Anaconda Company
660 Bannock Street
Denver, CO 80204

Mr. Edward E. Kennedy
Manager
Environmental Engineering
United Nuclear-Homestake Partners Corporation
P.O. Box 98
Grants, NM 87020

No. of Copies

OFFSITE

Mr. Archie LeGrand
Westinghouse Electric Corp.
Nuclear Fuel Division
P.O. Drawer R
Columbia, SC 29250

Dr. Jack Rothfleisch
U.S. Nuclear Regulatory Commission
Nuclear Materials, Safety and Safeguards
Washington, D.C. 20555

Mr. Charles Sanders
Manager
Radiation and Environmental Engineering
Westinghouse Electric Corp.
Nuclear Fuel Division
Drawer R
Columbia, SC 29205

Mr. William J. Shelley
Director
Regulation and Control
Kerr-McGee Nuclear Corp.
123 Robert S. Kerr Avenue
2205 McGee Tower
Oklahoma City, OK 73125

ONSITE

Pacific Northwest Laboratory

W. D. Felix
P. O. Jackson
10 D. R. Kalkwarf
J. C. Langford
J. Mishima
O. R. Moss
R. W. Perkins
L. C. Schwendiman
5 Technical Information
2 Publishing Coordination